NAVAL POSTGRADUATE SCHOOL

MONTEREY, CALIFORNIA

THESIS

POWER SAVINGS THROUGH ONBOARD ORBIT PROPAGATION FOR SMALL SATELLITES LIKE NPSAT1

by

David R. Hartmann

March 2016

Thesis Advisor: Daniel J. Sakoda
Co-Advisor: James A. Horning

Approved for public release; distribution is unlimited

THIS PAGE INTENTIONALLY LEFT BLANK

REPORT DOCUMENTATION PAGE	Form Approved OMB No. 0704–0188

Public reporting burden for this collection of information is estimated to average 1 hour per response, including the time for reviewing instruction, searching existing data sources, gathering and maintaining the data needed, and completing and reviewing the collection of information. Send comments regarding this burden estimate or any other aspect of this collection of information, including suggestions for reducing this burden, to Washington headquarters Services, Directorate for Information Operations and Reports, 1215 Jefferson Davis Highway, Suite 1204, Arlington, VA 22202-4302, and to the Office of Management and Budget, Paperwork Reduction Project (0704-0188) Washington, DC 20503.

1. AGENCY USE ONLY *(Leave blank)*	2. REPORT DATE March 2016	3. REPORT TYPE AND DATES COVERED Master's thesis

4. TITLE AND SUBTITLE POWER SAVINGS THROUGH ONBOARD ORBIT PROPAGATION FOR SMALL SATELLITES LIKE NPSAT1	5. FUNDING NUMBERS
6. AUTHOR(S) David R. Hartmann	
7. PERFORMING ORGANIZATION NAME(S) AND ADDRESS(ES) Naval Postgraduate School Monterey, CA 93943-5000	8. PERFORMING ORGANIZATION REPORT NUMBER
9. SPONSORING /MONITORING AGENCY NAME(S) AND ADDRESS(ES) N/A	10. SPONSORING / MONITORING AGENCY REPORT NUMBER

11. SUPPLEMENTARY NOTES The views expressed in this thesis are those of the author and do not reflect the official policy or position of the Department of Defense or the U.S. Government. IRB Protocol number ____N/A____.

12a. DISTRIBUTION / AVAILABILITY STATEMENT Approved for public release; distribution is unlimited	12b. DISTRIBUTION CODE

13. ABSTRACT (maximum 200 words)

The thesis investigates the feasibility of duty cycling the GPS receiver onboard small satellites like NPSAT1 in order to repurpose power savings in ways that would better serve the satellite's mission. Orbital propagation software run on onboard computer hardware produces accurate ephemeris data over short periods without continued GPS input. Longer periods relying on propagator ephemeris translate to greater power savings, but it also means increasing positional error. In order to better define the trade space between time and error of common propagators, Systems Tool Kit software was used to test the accuracy of the Two-Body and Simplified General Perturbations-4 propagators over time against positions measured by the Joint Space Operations Center. Two-Body propagators' error response varies as a function of altitude and inclination, with the worst case requiring GPS updates up to twice an orbit. Simplified General Perturbations-4 propagators' error depends strongly on the accuracy of the B* drag term, but is still sufficiently accurate to operate a day or more without a GPS update. Savings in the GPS power budget were found to exceed 96% and 99% for Two-Body and Simplified General Perturbations-4 propagators, respectively, and should be considered for use in future satellites.

14. SUBJECT TERMS NPSAT1, satellite, orbit propagation	15. NUMBER OF PAGES 77
	16. PRICE CODE

17. SECURITY CLASSIFICATION OF REPORT	18. SECURITY CLASSIFICATION OF THIS PAGE	19. SECURITY CLASSIFICATION OF ABSTRACT	20. LIMITATION OF ABSTRACT
Unclassified	Unclassified	Unclassified	UU

NSN 7540–01-280-5500 Standard Form 298 (Rev. 2–89) Prescribed by ANSI Std. 239–18

THIS PAGE INTENTIONALLY LEFT BLANK

Approved for public release; distribution is unlimited

POWER SAVINGS THROUGH ONBOARD ORBIT PROPAGATION FOR SMALL SATELLITES LIKE NPSAT1

David R. Hartmann
Lieutenant, United States Navy
B.S., Purdue University, 2010

Submitted in partial fulfillment of the
requirements for the degree of

MASTER OF SCIENCE IN SPACE SYSTEMS OPERATIONS

from the

NAVAL POSTGRADUATE SCHOOL
March 2016

Approved by: Daniel J. Sakoda
Thesis Advisor

James A. Horning
Co-Advisor

Rudy Panholzer
Chair, Space Systems Academic Group

THIS PAGE INTENTIONALLY LEFT BLANK

ABSTRACT

The thesis investigates the feasibility of duty cycling the GPS receiver onboard small satellites like NPSAT1 in order to repurpose power savings in ways that would better serve the satellite's mission. Orbital propagation software run on onboard computer hardware produces accurate ephemeris data over short periods without continued GPS input. Longer periods relying on propagator ephemeris translate to greater power savings, but it also means increasing positional error. In order to better define the trade space between time and error of common propagators, Systems Tool Kit software was used to test the accuracy of the Two-Body and Simplified General Perturbations-4 propagators over time against positions measured by the Joint Space Operations Center. Two-Body propagators' error response varies as a function of altitude and inclination, with the worst case requiring GPS updates up to twice an orbit. Simplified General Perturbations-4 propagators' error depends strongly on the accuracy of the B* drag term, but is still sufficiently accurate to operate a day or more without a GPS update. Savings in the GPS power budget were found to exceed 96% and 99% for Two-Body and Simplified General Perturbations-4 propagators, respectively, and should be considered for use in future satellites.

THIS PAGE INTENTIONALLY LEFT BLANK

TABLE OF CONTENTS

I. INTRODUCTION 1

II. SMALL SATELLITES 3
- **A. THE TRADE SPACE OF SMALL SATELLITES 4**
- **B. MISSION SETS 5**
  - **1. Space Science 5**
  - **2. Earth Observation 5**
  - **3. LEO Communications 5**
  - **4. Technology Demonstration 6**
  - **5. Training and Academic Education 7**

III. GLOBAL POSITIONING SYSTEM 9
- **A. SYSTEM ARCHITECTURE 9**
  - **1. Satellite Segment 9**
  - **2. Control Segment 10**
  - **3. User Segment 10**
- **B. BASICS 10**
- **C. ACCURACY AND ERROR 12**
  - **1. Ionosphere and Troposphere Errors 12**
  - **2. Clocks 12**
  - **3. Satellite Orbits 13**
  - **4. Multipath Propagation 13**
  - **5. Satellite Geometry 13**
- **D. AUGMENTATION 14**

IV. DESCRIBING ORBITS 15
- **A. SEMI-MAJOR AXIS (*a*) 16**
- **B. ECCENTRICITY (*e*) 17**
  - **1. Orbit Eccentricity Classifications 17**
    - ***a. Circular Orbit (e = 0) 17***
    - ***b. Elliptical Orbit (0< e <1) 18***
    - ***c. Parabolic Orbit (e = 1) 18***
    - ***d. Hyperbolic Orbit (e > 1) 18***
  - **2. Eccentricity Related to Cartesian Vectors 18**
- **C. INCLINATION (*i*) 18**
  - **1. Orbit Inclination Classifications 19**
    - ***a. Equatorial Orbit (i = 0) 19***
    - ***b. Prograde Orbit (0 < i < 90) 19***

c. Polar Orbit (i = 90) *19*
d. Retrograde Orbit (90 < i < 180) *19*
2. Inclination Related to Cartesian Vectors 19
D. RIGHT ASCENSION OF THE ASCENDING NODE (Ω) 20
E. ARGUMENT OF PERIGEE (ω) 21
F. TRUE AND MEAN ANOMALY 21

V. PROPAGATORS 23
A. TWO-BODY PROPAGATORS 23
B. J2 AND J4 PERTURBATION PROPAGATORS 24
C. SIMPLIFIED GENERAL PERTURBATIONS-4 PROPAGATOR 24
1. Two-Line Elements 25
2. SGP-4 Usage 26
D. HIGH PRECISION ORBIT PROPAGATOR 26
E. SUMMARY 26

VI. PROPAGATION EXPERIMENTS 29
A. EXPERIMENT SET UP 29
B. TWO-BODY PROPAGATOR 30
1. Altitude 30
2. Inclination 31
3. Eccentricity 33
4. Two-Body Propagation Summary 34
C. SGP-4 PROPAGATOR 40
D. SUMMARY 43

VII. APPLICATION 45
A. NPSAT1 45
B. EDISON DEMONSTRATION OF SMALL SATELLITE NETWORKS 48
C. ONBOARD PROPAGATION: NOT FOR EVERY MISSION 48
D. APPLICATION ON FUTURE SATELLITES 49

VIII. CONCLUSIONS AND FUTURE WORK 51

APPENDIX: SATELLITES BY EXPERIMENT 53

SUPPLEMENTAL 55

LIST OF REFERENCES 57

INITIAL DISTRIBUTION LIST 61

LIST OF FIGURES

Figure 1. Dilution of Precision as a Result of Satellite Geometry 14

Figure 2. Geocentric Equatorial Frame and the Orbital Elements 15

Figure 3. Two-Line Element Composition.....25

Figure 4. STK Propagator Summary of Forces.....27

Figure 5. Plot Expressing the Effect of Altitude on Two-Body Rate of Error.....31

Figure 6. Plot Expressing the Effect of Inclination on Two-Body Rate of Error 32

Figure 7. Nodal Regression Versus Inclination.....32

Figure 8. Plot Demonstrating the Minimal Effect of Altitude Relative to Inclination on Two-Body Rate of Error.....33

Figure 9. Plot Expressing the Effect of Eccentricity on Two-Body Rate of Error 34

Figure 10. Nodal Regression in Two-Body and SGP-4 Propagators.....35

Figure 11. Propagated Error Distance Between #23198 Obs 1 and Obs 2 and 13.....36

Figure 12. Error of the Two-Body Propagator with Consistent Measurement Locations.....37

Figure 13. Propagated Error Distance Between #22161 Obs 1 and Obs 8 and 9.....38

Figure 14. Error of the Two-Body Propagator with Inconsistent Measurement Locations.....39

Figure 15. Three Dimension Representation of Rate of Error as a Function of Inclination and Semi-Major Axis.....40

Figure 16. Plot Demonstrating the Variance Between TLEs 42

Figure 17. Plot of the First Term of the Best Fit Polynomial Versus the TLE Drag Term's Difference from the Most Accurate TLE's Drag Term.....43

Figure 18. Proposed Concept of Operations for Duty-Cycling GPS Receivers.....47

THIS PAGE INTENTIONALLY LEFT BLANK

LIST OF TABLES

Table 1. Classification of Small Satellites 3

Table 2. B* Difference Compared to LINEST 1st Term Values.....42

Table 3. NPSAT1 Average Power Usage Without Duty-Cycling GPS.....46

Table 4. NPSAT1 Average Power Usage With a 24-Hour Duty-Cycling Period of the GPS Receiver 46

THIS PAGE INTENTIONALLY LEFT BLANK

LIST OF ACRONYMS AND ABBREVIATIONS

ADCS	Attitude Determination and Control System
AFGP-4	Air Force General Perturbations-4 Propagator
AGI	Analytical Graphics Incorporated
AIAA	American Institute of Aeronautics and Astronautics
BOL	Beginning of Life
C/A	Coarse/Acquisition
CERTO	Coherent Electromagnetic Radio Tomography Experiment
CORS	Continuously Operating Reference Stations
COTS	Commercial Off-the-Shelf
CYGNSS	Cyclone Global Navigation Satellite System
C&DH	Command and Data Handler
DARPA	Defense Advanced Research Projects Agency
DOD	Department of Defense
EDSN	Edison Demonstration of Small Satellite Networks
EPS	Electric Power System
ESA	European Space Agency
FAA	Federal Aviation Administration
FOC	Final Operational Capability
GDGPS	Global Differential GPS
GEO	Geostationary Orbit
GNSS	Global Navigation Satellite System
GPS	Global Positioning System
HPOP	High Precision Orbital Propagator
IOC	Initial Operational Capability
JSPOC	Joint Space Operations Center
LEO	Low Earth Orbit
LQE	Linear Quadratic Equation
MCS	Master Control Station
MEO	Medium Earth Orbit
NASA	National Aeronautics and Space Administration

NAVSTAR	Navigation Satellite Timing and Ranging
NDGPS	Nationwide Differential GPS System
NGA	National Geospatial Intelligence Agency
NPS	Naval Postgraduate School
PANSAT	Petite Amateur Navy Satellite
RAAN	Right Ascension of the Ascending Node
SATCOM	Satellite Communications
SCORE	Signal Communications by Orbiting Relay
SGP	Simplified General Perturbation Propagator
SGP-4	Simplified General Perturbation Propagator No. 4
SMEX	Small Explorer Program
SMS	Solar Cell Measurement System Experiment
STK	Systems Tool Kit
TEC	Total Electron Content
TLE	Two-Line Element
UHF	Ultra-High Frequency
USSTRATCOM	United States Strategic Command
VISIM	Visible Wavelength Imager
WAAS	Wide Area Augmentation System

I. INTRODUCTION

Size has always been a major factor in space hardware. Bigger, heavier objects require larger, more expensive rockets to launch them. Advancements in micro-technology allow the use of increasingly smaller, lighter hardware to accomplish objectives and missions that would have been cost-inhibitive due to mass and size restrictions.

This trend has progressed to the point that size and weight are no longer the predominate factors hampering progress, but now the inability to generate adequate power on orbit on small satellites is a limiting feature. As the technology and ability to manufacture smaller and smaller items continues to make leaps and bounds, advancements in solar cell technologies have not kept up that pace.

Solar cells or an alternate technology will someday progress to provide sufficient power to small satellites. However, instead of patiently waiting for that technology to mature, satellite manufacturers and operators should produce creative solutions that make better use of the available power budget.

One such technique is to duty cycle the Global Positioning System (GPS) receiver to provide updates to an onboard orbit propagator. If equipped, most GPS receivers on small satellites only draw a few watts of power, but those few watts can be the difference in closing a communications link or accomplishing some other critical task.

In order to maximize the benefit of duty cycling a GPS receiver, it is important to understand the missions of small satellites and how propagators can relieve their dependence on the GPS system. This thesis starts by examining the pros and cons associated with using small satellites as well as their role in conducting space science, Earth observation, communications, technology demonstrations, and educational purposes. Then GPS will be discussed to provide an understanding of the system architecture and basic operation, as well as the factors limiting the accuracy of GPS and ways to augment the system to overcome those limitations. An overview of orbital elements and available propagators will provide the foundation for a careful examination

of how propagator accuracy degrades over time as a function of changing orbital elements. Ultimately, this analysis will lead to conclusions concerning the maximum safe length of time a propagator can operate between GPS updates, and consequently, the potential power savings available from duty cycling the GPS receiver.

II. SMALL SATELLITES

Since the first artificial satellite was launched in October 1957, satellites have become integral to the way the world operates. Satellites today can do everything from exploring deep space to delivering hundreds of television and music channels for entertainment. Historically, as the mission sets of satellites became more complex and demanding, the general size of these satellites also increased. The world's first manmade satellite, Sputnik I, was less than 58 cm in diameter and weighed only 84 kg [1]. Similarly, the first satellite the United States attempted to launch, Vanguard I, weighed less than 1.9 kg [2], a nanosat by today's standards as shown in Table 1. By comparison, the TerreStar-1, a communications satellite launched in 2009, has a wingspan of 32.3 meters and weighs 6910 kg [3]. These giants have proven their utility many times, but they are not without limitations caused by their size and cost. In the first 50 years of space launch, there were nearly 1600 micro-, nano-, and picosatellites launched into orbit [2]. Small satellites are often preferred to their larger cousins when mission requirements allow. Advances in micro-technology continue to evolve, allowing the small satellite's role in space to expand even further.

Table 1. Classification of Small Satellites

Small Satellite	500 - 1000 kg
Minisatellite	100 - 500 kg
Microsatellite	10 - 100 kg
Nanosatellite	1 - 10 kg
Picosatellite	0.01 - 1 kg
Femtosatellite	0.001 - 0.01 kg

Adapted from [4]: NASA. (2015). *About SSTP* [Online]. Available: http://www.nasa.gov/directorates/spacetech/small_spacecraft/smallsat_overview.html

Once reserved for the governments and militaries of well-developed countries, space continues to become increasingly accessible for new users. Commercial operators conscious of their financial "bottom line" strive to find the most beneficial balance between a satellite's capability and the overhead costs of building, launching, and operating a satellite. Academic institutions have only limited funding to provide

beneficial hands-on training to students. Even civil and military programs with constrained budgets can benefit from the use of small satellites without the price tag associated with larger satellites.

A. THE TRADE SPACE OF SMALL SATELLITES

Between 1962 and 1971, eight nations joined the United States and the Soviet Union as the only nations with satellites in orbit. Twenty of their first 31 satellites were microsatellites, including the first satellites for the United Kingdom, France, Australia, West Germany, and Japan. The remaining 11 were small satellites, all less than 264 kg [2]. There are many reasons these fledging space nations chose to launch smaller spacecraft as their initial foray into space, but most center on realities that still exist today. Small satellites are cheaper and easier to build than large satellites.

Of those first 31 launches, 14 were conducted using first- or second-generation indigenous rockets. The remaining launches either used small American Scout rockets or utilized larger Delta variants to deliver satellites to much higher orbits [2]. Launches are typically 30–40% of the total satellite cost, averaging nearly $10,000 per kg of payload [5]. This is the first advantage of small satellites: they require less thrust to launch into their orbits, meaning they can use a smaller rocket or even share a launch and the associated costs with another satellite. Additional material and developmental cost savings mean that small satellites can offer as much as 80% of the capability of larger satellites at a fifth of the cost [6].

However, there are applications and missions in which greater size is an advantage. Some missions will require the use of a larger satellite. Physical scaling has a direct effect on a number of factors that limit small satellites. Satellite power generation is directly dependent on the area of solar cells available. Small satellites have less surface area for body mounted solar cells and solar arrays, and subsequently cannot create as much power. In the field of optics, ground resolution at a given altitude varies as a function of the diameter of the primary reflector. In communications, larger antenna sizes yield better antenna gains for the transmission and reception of signals.

B. MISSION SETS

Small satellites fulfill roles across a wide range of applications. Space science, earth observation, communications, technology verification, and education are just a few of the mission fields that benefit from the use of small satellites.

1. Space Science

The flexible nature and short development time coupled with the financial advantages associated with small satellites make them ideal for budget-minded science experiments in space. In the 1980s, the National Aeronautics and Space Administration (NASA) started the Small Explorer (SMEX) Program with the Solar Anomalous Magnetospheric Particle Explorer to study the particles and cosmic rays in space. This was the first of 10 space science satellites in the SMEX program, four of which are still operating as of February 2016 [7]. The European Space Agency (ESA) also uses small satellites to conduct space science; including the 180 kg Solar Orbiter that will provide high-resolution images of the Sun from distances 80% closer than the Earth [8].

2. Earth Observation

Traditionally, satellites designed for Earth observation have required a large, heavy optical system in order to maximize resolution on the ground. In 2013, SkyBox launched the 100 kg SkySat-1, becoming the smallest satellite to achieve sub-meter resolution [9]. SkyBox aims to target a consumer base that can settle for their cheaper 0.9 m resolution over the much more expensive, albeit higher resolution, images of their competitors. SkySat-1 is the first of a 24-satellite constellation that will be built and launched to provide low-cost, high-definition imagery and video from Low Earth Orbit (LEO). SkyBox utilizes the CubeSat approach to satellite design and construction to minimize costs, accepting greater risk by cutting some redundancy and trading space-rated hardware for commercial off-the-shelf (COTS) hardware [9].

3. LEO Communications

When discussing communications satellites, many people think of large geostationary (GEO) spacecraft like the TerreStar-1 satellite or a Thuraya satellite. This

tendency overlooks the capability available from LEO constellations. The distance a signal has to travel to a LEO satellite is much shorter than to a GEO satellite, resulting in shorter time delays and less free-space loss in signal strength. However, it does take more satellites at LEO to constitute the same persistent coverage of a single GEO satellite.

In 1958, Defense Advanced Research Projects Agency (DARPA) launched the first communications satellite, a 45 kg Signal Communication by Orbiting Relay (SCORE) satellite, into a LEO orbit from Cape Canaveral, Florida [2]. Between 1964 and 1973, the Soviet Union launched over 380 small Strela satellites to build and maintain a LEO constellation for mobile communications. Most Strela satellites weighed only 61 kg and were stackable for launching multiples of up to eight at a time. Today, companies like ORBCOMM continue the heritage of small LEO communications satellites. The ORBCOMM constellation of 35, 46 kg satellites relay short data messages in a machine-to-machine (M2M) network that enables remote control and tracking of connected assets [2].

4. Technology Demonstration

The constant progressive march of technology allows satellite designers and manufacturers to incorporate significant new features and capabilities into each generation of new satellites. However, these untested technologies can represent significant risk if placed in a mission's critical path. The flexibility and low cost of small satellites allow developers to build a satellite with a number of these untested technologies, then launch and observe its performance in the space environment. If a technology fails, better it should happen on a cheap technology verification flight than on the expensive system for which it was ultimately designed.

In 2014, the United Kingdom launched the TechDemoSat-1 aboard a Soyuz rocket. The TechDemoSat-1 was designed to be an orbiting test bed for 25 new space technologies planned for the United Kingdom's NovaSAR satellite, NASA's Cyclone Global Navigation Satellite System (CYGNSS) satellite, and other commercial applications. These new technologies include advanced gyros and magnetometers for the Attitude Determination and Control System (ADCS) and an improved X-band downlink for high-speed communications [10].

5. Training and Academic Education

Relatively low costs and complexities of small satellites allows academic institutions like universities and even some high schools to budget a project where a group of students can design, build, and launch a satellite over the course of their academic careers. This concept was first realized in a cooperative effort between Utah State University and Weber State College to build the Northern Utah Satellite and launch it in 1985. Since then, the idea of using real satellites as a driver for engineering and operational education has proliferated worldwide.

At the Naval Postgraduate School (NPS) in Monterey, CA, the Small Satellite Design Program strengthens the Space Systems Engineering and Operations curricula by providing genuine mission requirements to students for them to design and build small satellite solutions. Standing at the intersection of the DOD and academia, NPS was a natural choice to sponsor a joint American Institute of Aeronautics and Astronautics (AIAA) and DARPA conference on lightweight satellites in 1987. The Small Satellite Design Program was a direct result of that conference [2].

The Small Satellite Design Program's first satellite project was Orion, which was designed to travel through the Van Allen radiation belts to take measurements. Although Orion was canceled due to lack of funding, it had proven its educational value at NPS. The follow-on project, the Petite Amateur Navy Satellite (PANSAT), was a store-and-forward Ultra-High Frequency (UHF) communications satellite. It was launched in October 1998 from the Space Shuttle Discovery [2].

NPSAT1 is the latest satellite built at NPS. Its primary mission is the education of NPS students, but once on orbit it will be a test bed for a number of technology demonstrations and experiments. From the beginning, the design of NPSAT1 has been interwoven with the Space Systems curricula [2]. Additionally, NPSAT1 is a consistent motivation for student research. To date, over 75 graduate theses have been written on Orion, PANSAT, and NPSAT1, proving that in addition to providing hands-on educational experience, these satellites encourage meaningful research that advances the field.

THIS PAGE INTENTIONALLY LEFT BLANK

III. GLOBAL POSITIONING SYSTEM

The Global Positioning System (GPS) is the United States' Global Navigation Satellite System (GNSS). GPS operates upon no less than 24 satellites at Medium Earth Orbit (MEO) providing millions of users globally with current position and velocity data on or above the Earth. GPS achieved Initial Operational Capability (IOC) in July 1993 after the 24th GPS satellite was launched, but Final Operational Capability (FOC) was not declared until July 1995 when the Department of Defense (DOD) finished military performance testing on the constellation [11]. Since then GPS has become integral in many aspects of modern technology. In 2015, the Global Navigation Satellite Systems Agency estimated there were over four billion devices worldwide using GPS to provide navigation and timing for everything from agriculture and financial institutions to complex United States military operations [12]. This section discusses only the basic principles and the necessary technical details about GPS. A more comprehensive discussion of the system can be found at www.gps.gov and information that is more technical can be found in the performance standards [13, 14].

A. SYSTEM ARCHITECTURE

Following the example set by GPS, all GNSS systems utilize a similar architecture consisting of a satellite segment operated and maintained by the control segment to deliver timing and ranging data to the user segment.

1. Satellite Segment

As of December 2015, there were 31 active Navigation Satellite Timing and Ranging (NAVSTAR) GPS satellites operating across six evenly distributed orbital planes at an altitude of 20,200 km [15]. The United States Air Force continues to purchase and launch increasingly robust and upgraded satellites to maintain and improve the constellation. GPS receivers require a signal from at least four satellites to determine position and velocity, but the current constellation strives to provide access to no less than six satellites at any time. In some cases, the signals from up to 10 satellites can be

received, allowing for increased positional accuracy through the selection of the strongest signals.

2. Control Segment

The GPS Master Control Station (MCS) is found at Schriever Air Force Base outside of Denver, Colorado. The alternate control station is located at Vandenburg Air Force Base, California. Additionally, the United States Air Force and the National Geospatial-Intelligence Agency (NGA) have several monitoring stations and ground antennas around the world to upload ephemeris data, perform orbital maintenance maneuvers, and observe satellite and signal health parameters [16].

3. User Segment

GPS receiver units are the enabling technology of a growing $26 billion/year market. There will be an estimated eight billion GPS receivers by 2020 [12]. Receivers have proliferated beyond navigation units in vehicles to ATMs, cell phones, and many other technologies. The Space Quest receiver used on NPSAT1 is slightly different from GPS devices in a car or cell phone, but utilizes many of the same concepts as Earth receivers.

Receivers used in terrestrial or airborne applications must determine position and velocity as independent variables through a technique called the 'snapshot least-square' method. In space, the laws of orbital mechanics relate a satellite's position and velocity; this allows use of a linear quadratic estimation (LQE), or Kalman filtering, to take multiple GPS measurements over time that can be used to more closely estimate the satellite's position and velocity as it progresses through its orbit [17].

B. BASICS

Each active satellite in the constellation transmits at least three ranging codes. The precision (P) code is the primary ranging code for the United States Military with enhanced security and jam resistance. The Y-code is used in anti-spoofing operations. Lastly, the civil ranging code, which is also the coarse/acquisition (C/A) code military receivers use to find and synchronize with the P or Y code and the principal signal in

civil ranging. A navigation message of uploaded satellite ephemeris data is added to the 1.023 MHz civil code and the 10.23 MHz military P(Y)-code. Older GPS satellites modulate the code-plus-data sequences for both C/A and P(Y) onto the L1 carrier (1575.42 MHz), but modulate only the P(Y) data sequence onto the L2 carrier (1227.6 MHz) before broadcasting L1 and L2 to the user community [18].

Starting in April 2014, Block IIR(M) and newer satellites began broadcasting civilian navigation data on the L2 carrier, allowing civilian receivers the benefit of a second signal to correct for ionospheric disturbances. The L2C signal allows civilian receivers to obtain accuracies approaching that of United States military systems. It is expected that the L2C signal will facilitate an additional $5.8 billion in economic productivity through the year 2030 [18]. Also in April 2014, Block IIF satellites began broadcasting the new L5 signal (1176.45 MHz), designed specifically for safety of life transportation. The L5 carrier frequency is inside the band of electromagnetic spectrum reserved solely for aviation safety. The L5 signal benefits from higher effective power, greater bandwidth, and an advanced signal design. Combined with the other civilian signals in a process called tri-laning, it is possible to achieve sub-meter accuracies without the use of augmentation systems. Tri-laning, similar to traditional wide-laning between the L1 and L2 signals, uses a combination of three signals to evaluate and eliminate the frequency-dependent errors such as those induced by ionospheric effects and multi-path propagation [19]. In 2016, the United States Air Force will begin launching Block III satellites capable of broadcasting a redesigned L1C signal that will allow for integration and cooperation between international satellite navigation systems like Europe's Galileo system, the Quasi-Zenith Satellite System of Japan, and China's Beidou system [18].

Each satellite continuously broadcasts its current position and exact time at 50 bits per second. GPS devices receive these messages from at least four satellites and solve a system of equations with four unknown variables: the three position coordinates and the exact time. The receiving device could generate time, but as the necessary atomic clocks are expensive and require a special environment, time is treated as an unknown variable.

In order to have the exact time information in the GPS device, the clocks must be synchronized [20].

C. ACCURACY AND ERROR

The performance standard of the civilian GPS signal is to provide positional accuracy with less than 7.8 m of user range error in 95% of all cases without any improvements [13]. In its quarterly report for April–June 2014, the Federal Aviation Administration (FAA) found that high-quality GPS receivers using the single L1 C/A signal could resolve position with less than 3.35 m of horizontal error and 4.68 m of vertical error 95% of the time [21]. Newer receivers taking advantage of the L2C signal and ionospheric correction will be much more accurate. The Space Quest Receiver onboard NPSAT1 advertises an accuracy of 10 meters, but above the ionosphere, the accuracy may be much better.

Despite the high level of sophistication in the GPS system, there are several possible sources of error still present in determining time and position, some of which follow.

1. Ionosphere and Troposphere Errors

The speed of the signal traveling through the ionosphere and troposphere is approximated as the speed of light. However, the ionosphere and the troposphere cause refraction and deceleration of the signal. During daylight hours, an increase in the ionosphere's Total Electron Content (TEC) due to solar radiation causes a delay of the signals propagating through it [22]. In legacy civilian receivers, this is the significant source of error; but with the use of a second frequency, this deceleration can be calculated and appropriate corrections applied [18].

2. Clocks

The atomic clocks onboard the satellites operate with cesium and rubidium oscillators that produce a small error of approximately 10^{-8} seconds per day. This corresponds to approximately 3.5 meters if the satellite is not updated for 24 hours.

Updating occurs every 12 hours on average, therefore the positional error caused by the satellite's clock would be expected to be less than 1–2 meters [23].

3. Satellite Orbits

The ephemeris data of a GPS satellite is measured from the ground and uploaded to the satellite. This process is accurate only to a few meters, but the position of the satellite is a fundamental piece of information broadcasted to user receivers and errors in satellite position translate into errors in calculated receiver position [23].

4. Multipath Propagation

When the receiver picks up signals reflected off buildings and other surfaces, it cannot account for the additional time and distance that signal traveled. This introduces a higher pseudo-range that makes the receiver believe it is further from the satellite, thereby degrading accuracy [23].

5. Satellite Geometry

If the receiver is using signals from four satellites with low angular separation, it is more difficult to calculate a precise solution. Using the worst case as an illustration, the receiver would receive four signals having traveled nearly the same distance from nearly the same azimuth, creating four very similar and overlapping spheres of positional possibility. As shown in Figure 1, as angular separation between the broadcasting satellites approaches right angles, the ability of the receiver to accurately resolve its position also increases [24].

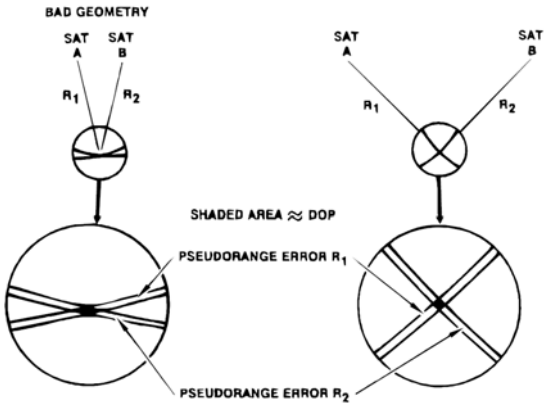

Figure 1. Dilution of Precision as a Result of Satellite Geometry

Source [24]: USCG. (1996). *NAVSTAR GPS user equipment introduction* [Online]. Available: http://www.navcen.uscg.gov/pubs/gps/gpsuser/gpsuser.pdf

D. AUGMENTATION

If higher accuracy is required, there are several augmentation systems available. These include the Wide Area Augmentation System (WAAS), Nationwide Differential GPS System (NDGPS), Global Differential GPS (GDGPS), and Continuously Operating Reference Stations (CORS). These systems use receivers at surveyed positions on the Earth to apply an error correction to the received GPS signal and transmit that information to capable receivers directly, like the DGPS systems, or indirectly, like the WAAS system that utilizes geostationary satellites to relay the information [25, 26, 27].

IV. DESCRIBING ORBITS

The position, velocity, and time information that can be retrieved from an onboard GPS receiver allows a satellite's onboard processor to calculate the Cartesian element vectors that define its orbit [17]. These three-dimensional vectors are convenient for computations such as propagation, but are less helpful in describing the orbit. The six orbital elements are an important piece of Two-Line Elements (TLE) used by the United States Strategic Command (USSTRATCOM) to describe the orbits of the space objects it tracks and is a common language amongst those who operate and track satellites in space. Orbital elements can be expressed by converting the Cartesian vectors using relationships defined by the laws of orbital motion. The following is provided only as a basic reference of the orbital elements pertinent to orbital propagation. For a more complete discussion of orbital mechanics, see reference [28]. Figure 2 is a visual representation of the orbital elements described.

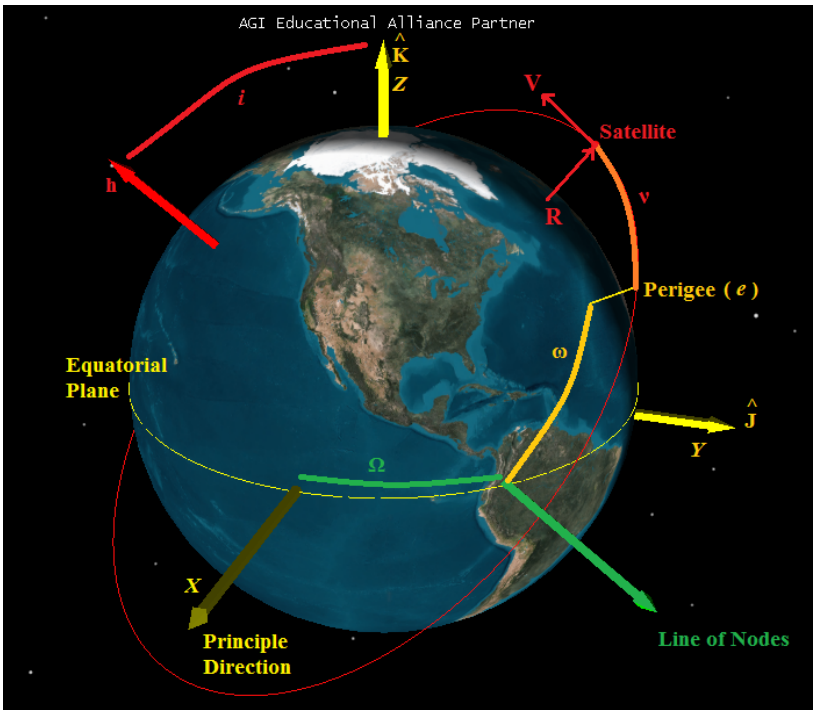

Figure 2. Geocentric Equatorial Frame and the Orbital Elements

Adapted from [29]: *Systems Tool Kit*, version 10.1.0. Analytical Graphics, Incorporated, Exton, PA, 2016.

A. SEMI-MAJOR AXIS (*a*)

An orbit's size is often measured by its semi-major axis. The major axis is the long axis of an ellipse; the semi-major axis is half that length. It relates directly to the satellite's specific mechanical energy. Because of this, the semi-major axis can be derived from a given position and velocity via a GPS receiver. Terrestrial and airborne GPS receivers typically output latitude, longitude, and an altitude, but receivers designed for spacecraft output the Cartesian vectors for position and velocity [17].

Starting with a position and velocity vectors measured from the center of the Earth, this equation can be used to determine the specific mechanical energy [28]:

$$\varepsilon = \frac{V^2}{2} - \frac{\mu}{R} \tag{1}$$

where

ε = specific mechanical energy (km^2/s^2)

V = magnitude of the spacecraft's velocity vector $\vec{V}$ (km/s)

R = magnitude of the spacecraft's position vector $\vec{R}$ (km)

μ = gravitation parameter of Earth (398600 km^3/s^2).

The satellite's specific mechanical energy is used to describe the semi-major axis:

$$a = -\frac{\mu}{(2 \times \varepsilon)} \tag{2}$$

where

a = semi-major axis (km).

Therefore, the semi-major axis is directly related to position and velocity through the following relationship [27]:

$$a = \frac{-\mu}{V^2 - \left(\frac{2\mu}{R}\right)} \tag{3}$$

In Two-Line Elements, mean motion, or the number of revolutions a satellite makes in a solar day, represents the semi-major axis. To determine the semi-major axis from mean motion, solve first for the orbital period, or the amount of time the satellite takes to make one revolution [28]:

$$T = \frac{86400}{M} \tag{4}$$

where

T = orbital period (seconds)

M = mean motion (revolutions/day)

and 86400 is the number of seconds in one solar day.

Then use the following relationship to solve for the semi-major axis:

$$T = 2\pi\sqrt{\frac{a^3}{\mu}} \tag{5}$$

B. ECCENTRICITY (*e*)

The eccentricity of an orbit specifies its shape by examining the ratio of the distance between the two foci and the distance from perigee to apogee [28].

$$e = \frac{2c}{2a} \tag{6}$$

where

c = half the distance between the foci of the ellipse.

1. Orbit Eccentricity Classifications

There are four classes of eccentricity to describe an orbit.

a. Circular Orbit (e = 0)

Circular orbits have equal semi-major and semi-minor axes. A satellite's motion around a circular orbit is of uniform velocity. In practice, the external forces that act on a

satellite make it impossible to achieve a perfectly circular orbit; however, nearly circular orbits can be maintained with eccentricities less than 0.0001.

b. Elliptical Orbit (0< e <1)

Objects in an elliptical orbit have non-uniform velocities. At apoapsis, the point furthest from the parent body, the object moves slowest and gradually increases velocity until reaching periapsis, the point closest to the parent body. This is consistent with Kepler's second law, which states an object in orbit sweeps out equal area in equal sums of time [30].

c. Parabolic Orbit (e = 1)

A parabolic orbit describes an object with the minimum energy to escape the gravitational pull of the parent body.

d. Hyperbolic Orbit (e > 1)

A hyperbolic orbit has excess energy to escape a parent body's gravitational pull. These orbits are useful for planning a "sling-shot" maneuver to gain additional velocity, like NASA's Voyager missions [31].

2. Eccentricity Related to Cartesian Vectors

Eccentricity can be related to position and velocity in the form of a vector that points from the center of the Earth to the perigee of the orbit. The vector $\vec{e}$ is unitless, but of magnitude e [28].

$$\vec{e} = \frac{1}{\mu}[(\mathrm{V}^2 - \frac{\mu}{R})\vec{R} - (\vec{R}\cdot\vec{V})\vec{V}] \tag{7}$$

C. INCLINATION (*i*)

The inclination of an orbit describes the angle between the equatorial and orbital planes. It is often referred to as the tilt of the orbit.

1. Orbit Inclination Classifications

Inclination is defined from zero to 180 degrees (zero to π radians). Satellite inclinations can be categorized into one of four classifications.

a. Equatorial Orbit ($i = 0$)

Objects in an equatorial orbit are always above the equator. Geostationary satellites utilize this characteristic to minimize movement north and south, allowing the terrestrial antennas they communicate with to remain fixed [32].

b. Prograde Orbit ($0 < i < 90$)

A prograde orbit moves in the same direction as the spin of the Earth, to the East [32].

c. Polar Orbit ($i = 90$)

Polar orbits are most useful for missions that require the satellite to cover all of the Earth. By flying perpendicular to it, this orbit also minimizes the J2 effect, a significant perturbation caused by the Earth's oblateness around the equator [28].

d. Retrograde Orbit ($90 < i < 180$)

Satellites in a retrograde orbit move counter to the spin of the Earth, to the West. A popular subset of retrograde orbits is the sun-synchronous orbit that is often used in remote sensing. These orbits are designed to utilize nodal regression to match the Earth's orbit around the Sun. This allows the satellite to pass over a latitude at the same time of day, keeping sun angles and shadows consistent between observations [32].

2. Inclination Related to Cartesian Vectors

In order to relate the inclination to the Cartesian vectors, it is useful to first define the specific relative angular momentum of a satellite. Specific relative angular momentum, $\vec{h}$, is the cross product of the position $\vec{R}$ and velocity $\vec{V}$ vectors. Visually, $\vec{h}$ will always be perpendicular to both the $\vec{R}$ and $\vec{V}$ vectors in accordance with the Right-Hand Rule. This also means that for an equatorial orbit $\vec{h}$ will be parallel with the

Earth's spin axis, a unit vector defined $\hat{K}$. It follows that any inclination (i) is equal to the angular difference between vectors $\vec{h}$ and $\hat{K}$, and that relationship is defined as per equation (8) [28].

$$i = \cos^{-1}\left(\frac{\hat{K}\cdot\vec{h}}{Kh}\right) \tag{8}$$

where

$\hat{K}$ = unit vector in the direction of Earth's north polar axis (+Z)

K = magnitude of $\hat{K}$ = 1

h = magnitude of $\vec{h}$ (km^2/s).

D. RIGHT ASCENSION OF THE ASCENDING NODE (Ω)

The Right Ascension of the Ascending Node (RAAN) is an orbit's rotation in the equatorial plane with respect to the principal direction, or its swivel. It is described by measuring the angle between the Earth-Sun vector during the vernal equinox to where the orbit crosses the equatorial plane moving northward, the ascending node [32]. This point can be calculated through the cross product of the (K) and (h) vectors as in equation (9). Equation (10) shows how the RAAN is the angular separation between $\vec{n}$ and the principle direction $\hat{I}$ [28].

$$\vec{n} = \hat{K}\times\vec{\mathrm{h}} \tag{9}$$

where

$\vec{n}$ = ascending node vector km^2/s, points at ascending node)

$$\Omega = \cos^{-1}\left(\frac{\hat{I}\cdot\vec{n}}{n}\right) \tag{10}$$

where

Ω = RAAN (degrees or radians)

$\hat{I}$ = unit vector in the principal direction (Earth-Sun vector at the vernal equinox)

$\vec{n}$ = ascending node vector (km^2/s)

n = scalar magnitude of $\vec{n}$ (km^2/s).

E. ARGUMENT OF PERIGEE (ω)

The argument of perigee for non-circular orbits is the angular displacement between the ascending node and the point of perigee, measured in the same direction as spacecraft motion [32]. Recall the vector $\vec{e}$ points from the center of the Earth to the orbit's perigee; in order to distinguish ω between quadrants, there are two equations. If $\vec{e}$ points above the equator, use equation (11); if $\vec{e}$ points below the equator, use equation (12) [28].

$$\omega = \cos^{-1}\left(\frac{\vec{n}\cdot\vec{e}}{ne}\right), \vec{e}_z \geq 0 \tag{11}$$

$$\omega = 360 - \cos^{-1}\left(\frac{\vec{n}\cdot\vec{e}}{ne}\right), \vec{e}_z < 0 \tag{12}$$

F. TRUE AND MEAN ANOMALY

The previous orbital elements have defined the orbit; the remaining task is to define where a satellite is along its orbit at a given time. True anomaly describes the angle between the orbit's perigee vector $\vec{e}$ and the satellite's position vector $\vec{R}$, measured along the path of motion [29, 33].

$$\nu = \cos^{-1}\left(\frac{\vec{e}\cdot\vec{R}}{eR}\right) \tag{13}$$

where

ν = true anomaly.

In elliptical orbits, the angular rate of change of a satellite's true anomaly varies directly with its velocity. This cyclical variation makes it impossible to solve for true anomaly analytically as a function of time. The solution is to superimpose a circular orbit with the same orbital period as the original orbit. Kepler's second law dictates that both orbits sweep equal areas in equal times; but the circular orbit sweeps at a constant angular

rate and is analytically solvable. This constant angular rate is called the mean motion and the position of the object along this circular orbit is called the mean anomaly [28]. TLEs annotate mean anomalies to describe a satellite's location in its orbit at the prescribed epoch for use in SGP propagators.

V. PROPAGATORS

There are many types of propagators, each with a varying degree of complexity and accuracy in their approach to modeling orbits. Most utilize a combination of analytical and numerical integration methods to calculate the movement of a satellite through its orbit. Analytical propagators make use of well-founded assumptions to simplify the orbital model such that a closed-form solution of position and velocity can be calculated directly. Numerical integration models account for the effect of more forces acting on a satellite over very short periods of time, but due to the complexity of the math involved, produce only a close approximation of the solution. When choosing a propagator, there is an important trade to consider between accuracy and computational demands. A simpler analytical propagator, like a two-body model, might be overlooked at first due to its inaccuracy over time, but may appear more attractive in the face of the cost and hardware size restraints imposed by more computationally rigorous numerical integration propagators.

The propagators discussed refer to the propagators available in Analytical Graphics, Inc.'s (AGI) System Tool Kit (STK). Other propagators of a similar name are available online; it can be expected that most features will be similar to these, although not necessarily identical.

A. TWO-BODY PROPAGATORS

Two-body propagators use the most assumptions of any model to simplify the highly complex movement of satellites. By assuming the smaller forces that act on a satellite are negligible compared to the force of the Earth's gravity, the difficult mathematics involved in accounting for these forces is greatly reduced. The forces that are assumed negligible include the drag on a satellite traveling through the Earth's atmosphere, third-body gravitational forces like those caused by the Sun and the Moon, and the acceleration due to pressure from solar radiation and electromagnetic fields. It is also assumed that, compared to the satellite, the Earth is a much larger mass of uniform density. This allows the propagator to disregard the small changes in the gravitational

field around Earth and the small gravitational force of the satellite on Earth. The final assumption is that the satellite is not maneuvering or thrusting in any direction [33].

These assumptions allow the simulation to use a mostly analytical approach to define the orbit. Numerical integration is still necessary to determine the satellite's true anomaly via Kepler's Equation [34].

B. J2 AND J4 PERTURBATION PROPAGATORS

The oblate spheroid shape of the Earth causes a non-uniform gravitational field with stronger forces along the equatorial belt where the Earth is widest. This force, called the J2 effect, is the largest perturbation force on most LEO satellites [35]. J2 Propagators model the first order secular effect on an orbit's argument of perigee, RAAN, and the mean motion. J4 Propagators model the first and second order effects of the J2 perturbation and the first order of the J4 effect, another zonal coefficient relating to the gravitational acceleration at a given point. However, because the force due to J4 is approximately 1000 times less than J2, the two propagators produce very similar results for short simulations [33]. Additional calculations used in J4 only begin to make a marked difference over the course of longer simulations.

C. SIMPLIFIED GENERAL PERTURBATIONS-4 PROPAGATOR

The space and defense division of the Ford Motor Company, Aeronutronic Systems, Inc., developed the first SGP Propagator in the late 1960s based upon the work of Max Lane in 1965. In 1969, Max Lane and Ken Cranford completed follow-on work on a propagator that would become the Air Force General Perturbations-4 (AFGP-4) propagator. In order to ease computational requirements, the AFGP-4 propagator's accuracy was sacrificed to reduce complexity. An intermediate propagator simplified the effect of drag by only evaluating the secular terms, but maintained the full gravitational model designed by Brouwer in 1959. Simplified General Perturbations #4 (SGP-4) goes one step further by assuming small eccentricities in the Brouwer model, thereby simplifying much of the computations [36].

The 14th Aerospace Force implemented their new propagation theory, SGP-4, into the Cheyenne Mountain Complex computers in the early 1970s to better support the mission to maintain a catalog of all space objects. Within the same decade, SGP-4 would be further upgraded to better tackle third body gravity effects upon deep space orbits [37].

1. Two-Line Elements

Two-line element sets have been used by the United States Air Force in orbital propagation calculations since 1965 and are the only inputs to the SGP-4 propagator. The format was created to be a standard that could be punched into data cards and fed into early computers. As technology has increased over time, the TLE has remained the format of choice to express orbital data.

Each of the two lines in an element set is 69 characters long. The first line identifies the satellite, lists the time the observation was taken, the first and second derivative denoting change in mean motion, and the B* term. B* is the product of one-half the satellite's ballistic coefficient and the atmospheric density reference value (ρ) [38] and is critical to the way SGP-4 calculates the effect of drag on the satellite. The second line of the TLE expresses the six orbital elements [39]. Figure 3 shows how the pieces of the two-line element are organized.

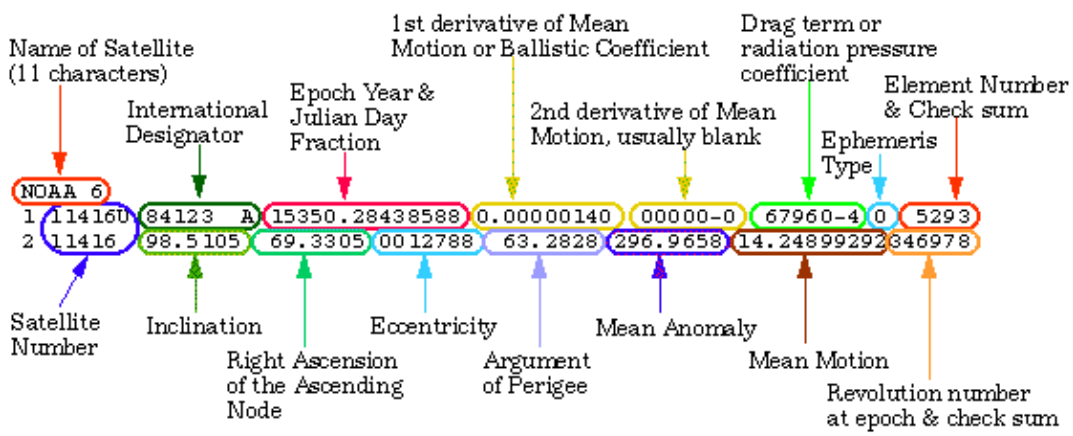

Figure 3. Two-Line Element Composition

Source [39]: NASA. (2011). *Definition of two-line element set coordinate system* [Online]. Available: http://spaceflight.nasa.gov/realdata/sightings/SSapplications/Post/JavaSSOP/SSOP_Help/tle_def.html

2. SGP-4 Usage

SGP-4 is a common propagator among amateur and professional satellite observers and operators. It strikes a balance between accuracy and computational requirements, making it a good candidate for use in onboard satellite propagation. The code is available free in multiple software languages online and using the TLEs available through Space-Track.org, anyone can have access to a reliable propagator without incurring additional costs. To its detriment, relying upon a TLE can introduce additional delays. JSPOC does not produce and publish TLEs at regular intervals, as it is limited to when the object is within sight of its equipment.

As long as the satellite has a functioning GPS receiver producing a state vector, it would be advantageous to input that state vector into a propagator with similar atmospheric and gravitational models as SGP-4. This will provide for instantaneous updates upon demand.

D. HIGH PRECISION ORBIT PROPAGATOR

An example of a numerical integration propagator is the High Precision Orbit Propagator (HPOP). It utilizes numerical integration in order to accommodate highly complex models of the perturbing forces. These include a scrupulous representation of the zonal coefficients of Earth's gravity, a highly accurate model of solar and lunar gravity derived from data from the U.S. Naval Observatory, an atmospheric drag model that accounts for the variations due to solar heating, and solar radiation pressure. HPOP can maintain accuracies of about of 10 meters per orbit, but is a heavy burden on computational power and is not freely available to developers and satellite operators like the propagators mentioned earlier [33].

E. SUMMARY

Figure 4 shows the capability of the different propagators to account for the various forces that act on Earth satellites. The accuracy of the propagator can be tied to how many of these forces it can model; however, these forces are increasingly small and make less significant contributions to overall accuracy.

Tracking satellites from the ground allows use of greater computational and power resources than are available to a satellite while on orbit. The increased accuracy is useful for orbital planning pre-launch, and conjunction analysis and maneuver planning post-launch. In space, a satellite is constrained to the power generation and processing hardware with which it was launched and was designed to accomplish its assigned mission. Again, the goal of this thesis was to explore potential energy savings using propagators to the maximum extent possible, but the higher end propagators quickly approach the limit where the burden and cost of development and implementation outweigh the benefits gained through power savings.

	Propagators Accounting for Forces Acting on an Earth Orbiting Satellite					
	Earth Gravity	**Earth Atmosphere**	**J2**	**J4**	**Third Body Gravity**	**Solar Radiation Pressure**
Approx. Order of Magnitude of Accel. for Satellites 300-1200 km	10^{-2} km/s^2 Decreasing with Altitude	10^{-4}-10^{-13} km/s^2 Decreasing with Altitude	10^{-5} km/s^2 Decreasing with Altitude	10^{-7} km/s^2 Decreasing with Altitude	10^{-9} km/s^2 Increasing with Altitude	10^{-10} km/s^2 Increasing with Altitude
Two-Body	■					
J2	■		■			
J4	■		■	■		
SGP-4	■	■	■	■	■	
HPOP	■	■	■	■	■	■

Figure 4. STK Propagator Summary of Forces

Adapted from: [34] E. Fantino. (2011). *Orbits and propagators* [Online]. Available: https://www.agi.com/resources/educational-alliance-program/curriculum_exercises_labs/ETSEIAT_2011_2012/DVE1_2011_T07__Orbits_STK.pdf; [34] O. Montenbruck and E. Gill, *Satellite Orbits: Models, Methods, Applications,* 3rd ed. Germany: Springer-Verlag, 2005.

THIS PAGE INTENTIONALLY LEFT BLANK

VI. PROPAGATION EXPERIMENTS

In order to ascertain the potential power savings achieved by duty cycling the GPS receiver, first it must be determined how quickly a propagator's uncertainty grows to an accepted level. Beyond that level, the GPS receiver must provide a new position update or risk reducing mission effectiveness by introducing positional uncertainty.

Of the classic elements that define an orbit, only semi-major axis and eccentricity change the shape of an orbit, inclination, RAAN, and the argument of perigee only speak to its orientation. However, inclination directly influences how the satellite is affected by the J2 effect. For this reason, the accuracy of the two-body and SGP-4 propagators were tested over time by varying these three variables: semi-major axis, inclination, and eccentricity.

A. EXPERIMENT SET UP

The Joint Space Operations Center (JSPOC) catalog of satellites available at www.space-track.org was downloaded and sorted by mean motion, inclination, and eccentricity to identify three groups of satellites for testing. To test the effect of each element singularly upon a propagator, each group was comprised of up to thirty objects with similar values in two elements and distributed values for the third, varying element. Appendix A lists the objects chosen by test group organized by the variable element.

For this experiment, the TLEs taken from JSPOC via www.space-track.org are accepted as measured, accurate observances of the object's position at the noted epoch. This assumption may overstate the actual accuracy of JSPOC's TLEs, estimated at approximately one kilometer [40]. The TLEs for the period between November 30 and December 8, 2015 were downloaded and input as the ephemeris data for separate SGP-4 satellites using STK 10.1.0. Corresponding ephemeris data was used to create two-body satellites. The TLEs and corresponding two-body ephemeris data are listed by its satellite catalog number in the Supplemental.

With each STK satellite representing a measured position at a designated epoch, every satellite was propagated to the epoch times of each later observation and distance

between the two satellites was measured and recorded. The recorded error measurements for the SGP-4 and two-body experiments are listed by their satellite catalog number in the Supplemental.

B. TWO-BODY PROPAGATOR

Error for the two-body propagator was found to increase at a linear rate over time; however, the rate of change, the slope of that linear rate, varied as a function of altitude and inclination. Plots demonstrating these linear increases can be found for each satellite in the Supplemental.

1. Altitude

To test the effect of altitude on a two-body propagator, 27 near-circular, mostly polar orbits over varying semi-major axes were propagated over the course of no more than one week. This group of satellites has eccentricities less than 0.01 in order to keep the exposure to the atmosphere mostly constant through the satellite's entire orbit. Satellite inclinations between 80 and 100 degrees minimized the contribution of error introduced by the forces related to the oblateness of the Earth. To evenly distribute satellites according to altitude, there are at least three satellites per 100 km of altitude over the range of 350 km to 1200 km.

The rate of error over time was found to have a strong correlation with the altitude of the object. Figure 5 shows that, with a few exceptions, the rate of error decreases at a nearly linear rate of approximately 0.56 km/hour per 100 km of altitude increase. It is not surprising that altitude would have such a pronounced effect on accuracy in a two-body propagator because these propagators do not account for atmospheric drag. However, further investigation is required to determine why the rate of error appears to have a linear response instead of the exponential decay corresponding with the force of the atmosphere as a function of altitude.

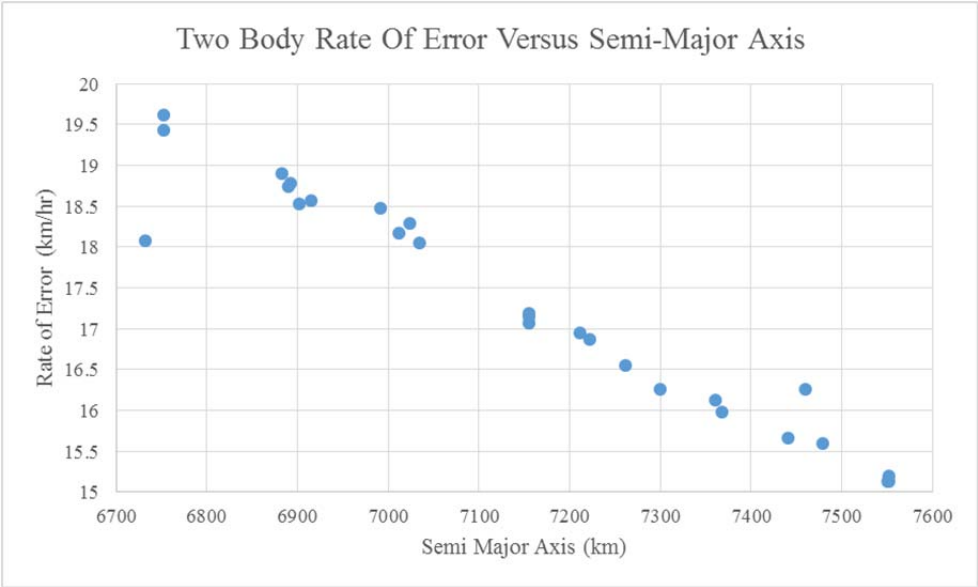

Figure 5. Plot Expressing the Effect of Altitude on Two-Body Rate of Error

2. Inclination

The effect of inclination was tested by propagating 30 objects of inclinations between the range zero to 100 degrees with eccentricity less than 0.01 and orbiting above most of the atmospheric drag at 500 to 875 km altitude. At least three satellites represent each 10-degree increment from zero to 100 degrees. By holding the altitude mostly constant, the changes due to atmospheric drag and third body gravity are equally constant, leaving the J2 effect as the predominant uncontrolled variable. Accordingly, the slope of the individual satellite two-body propagation errors, signifying rate of error, plotted as a function of inclination in Figure 6 has a similar shape as the nodal regression by inclination plot shown in Figure 7. Figure 8 is the same set of error rates plotted as a function of altitude. There is significantly less correlation to altitude, showing that inclination is the dominant factor. The plots of Figure 7 reinforce the findings of the altitude and inclination study; notice the decrease in nodal regression with the increase of altitude and inclination.

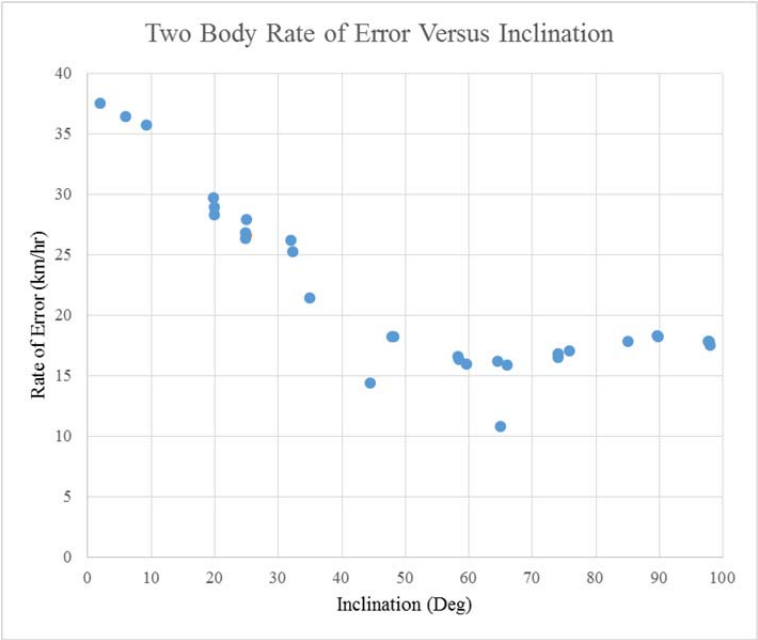

Figure 6. Plot Expressing the Effect of Inclination on Two-Body Rate of Error

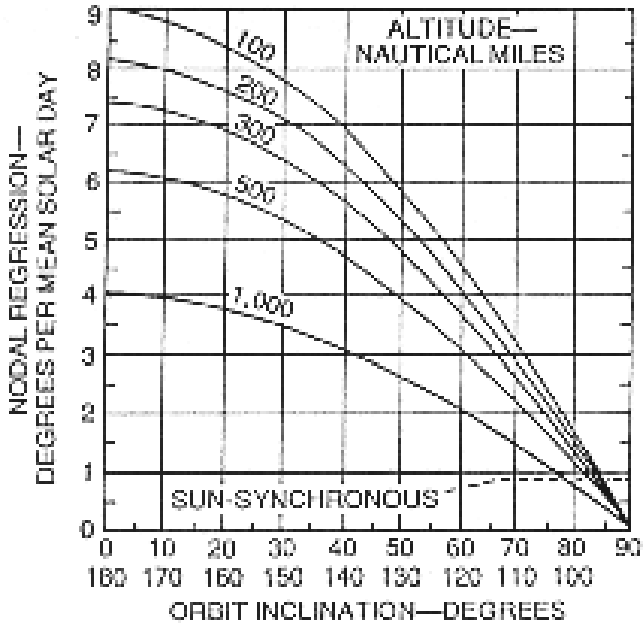

Figure 7. Nodal Regression Versus Inclination

Source: [41] M. J. Muolo, *Space Handbook,* vol. 2, Maxwell AFB, AL: Air University, p. 26, 1993. Note: This plot is in nautical miles, this experiment was conducted with satellites between 500–875 km, or 267–450 nm.

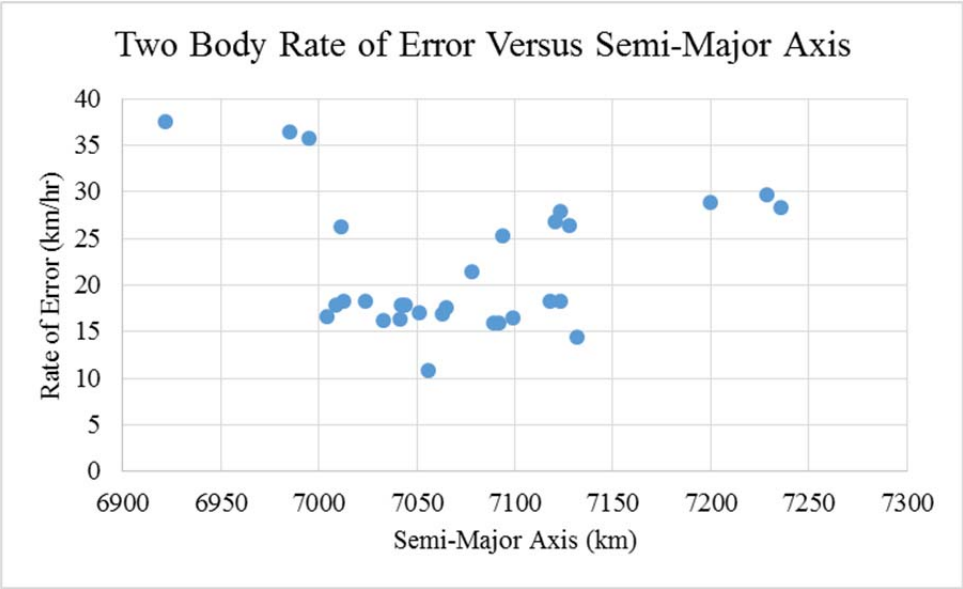

Figure 8. Plot Demonstrating the Minimal Effect of Altitude Relative to Inclination on Two-Body Rate of Error

This is the same rate of error data plotted against corresponding satellite altitudes. This plot demonstrates significantly less correlation than when plotted against inclination.

3. Eccentricity

Thirty satellites with eccentricities spread across the range zero to 0.1, with semi-major axes between 7500 km and 7600 km and inclinations between 56 and 74 degrees were propagated in a similar fashion as the previous test groups. The range zero to 0.1 was chosen as it represents an overwhelming majority of the space catalog and was deemed a sufficient representation of the orbits in which small satellites would likely operate. However, as shown in Figure 9, there was no discernable pattern relating the rate of error to increasing eccentricity. Instead, these rates were consistently between 10 and 14 km/hr, seeming to correspond more closely with their altitude and inclination as previously discussed. This phenomenon is absent in the SGP-4 propagator because it accounts for gravity's zonal harmonics.

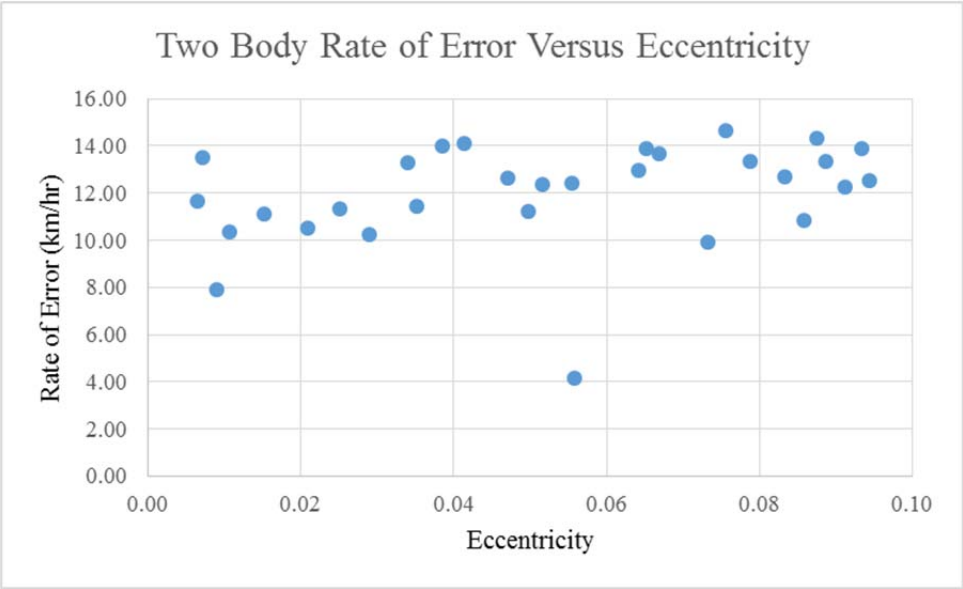

Figure 9. Plot Expressing the Effect of Eccentricity on Two-Body Rate of Error

4. Two-Body Propagation Summary

The strong correlations found between the rate of error and changes in altitude and inclination are not surprising as they can be easily tied to perturbations that the propagator assumes as negligible in the name of simplicity. Prior to testing, it was anticipated that changes in eccentricity would cause some detectable change in error rate due to non-uniform exposure to atmospheric forces. However, this was shown to be a non-issue and eccentricities between zero and 0.1 do not play a significant role in two-body propagator error.

All of the error measurements were taken at the epoch of the later TLE. However, if both modeled satellites are propagated together over time a sinusoidal element becomes apparent in the error between the two. This is caused by the nodal regression associated with the J2 effect. Nodal regression, measured in degrees, translates into the largest error distance at the equator and the smallest error distance at the orbit's latitudinal extremes as shown in Figure 10.

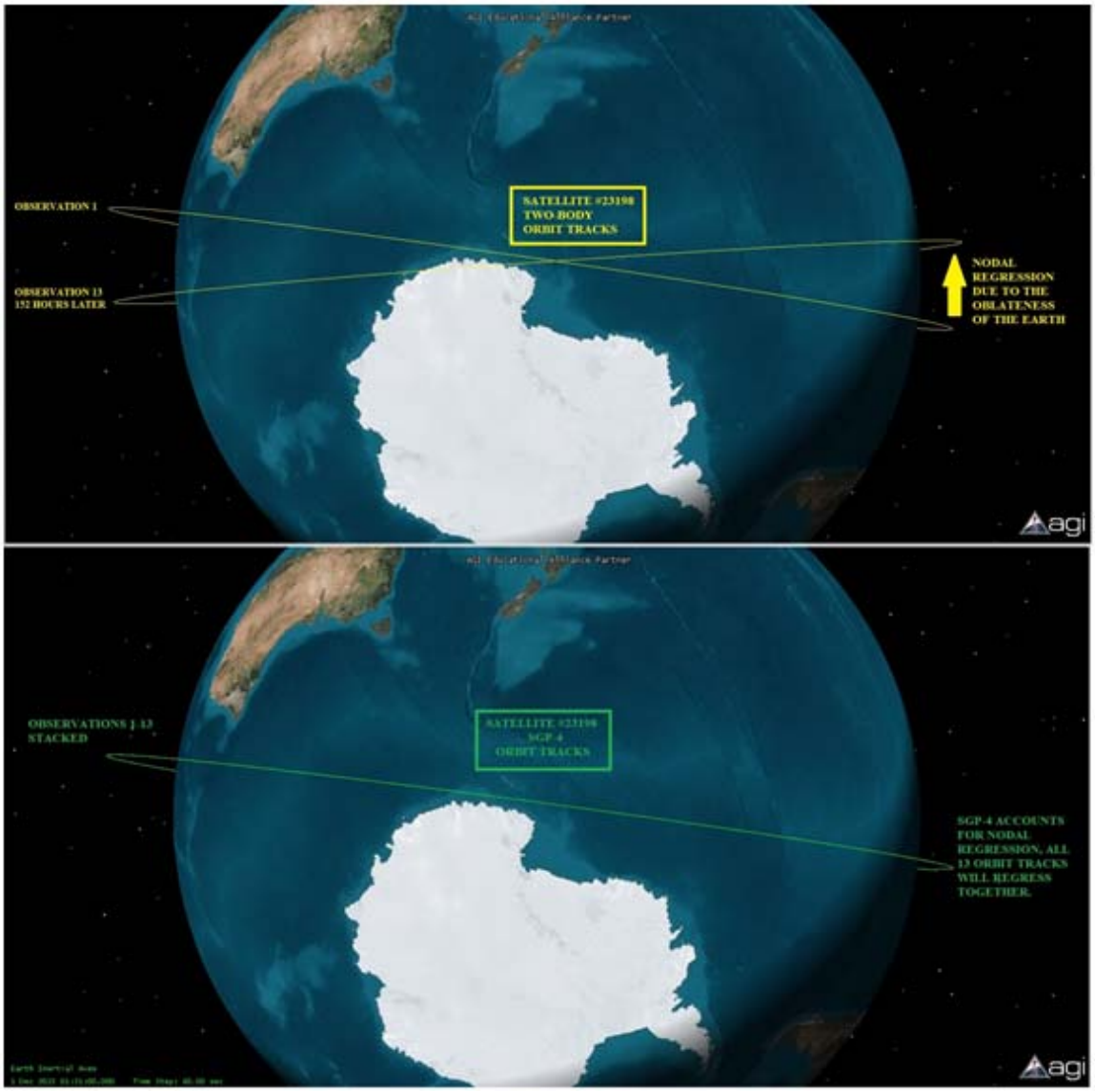

Figure 10. Nodal Regression in Two-Body and SGP-4 Propagators

Adapted from [29]: *Systems Tool Kit*, version 10.1.0. Analytical Graphics, Incorporated, Exton, PA, 2016.

All of this emphasizes the importance of using TLEs measured at similar points in a satellite's orbit. When all the measurements were observed at a consistent point, the error rate plots represent a single line. Most of the satellites used in this experiment follow this trend. Notice how epochs for Satellite #23198 were generated at similar points in the sinusoidal plots of Figure 11, this translated into the linear response demonstrated in Figure 12.

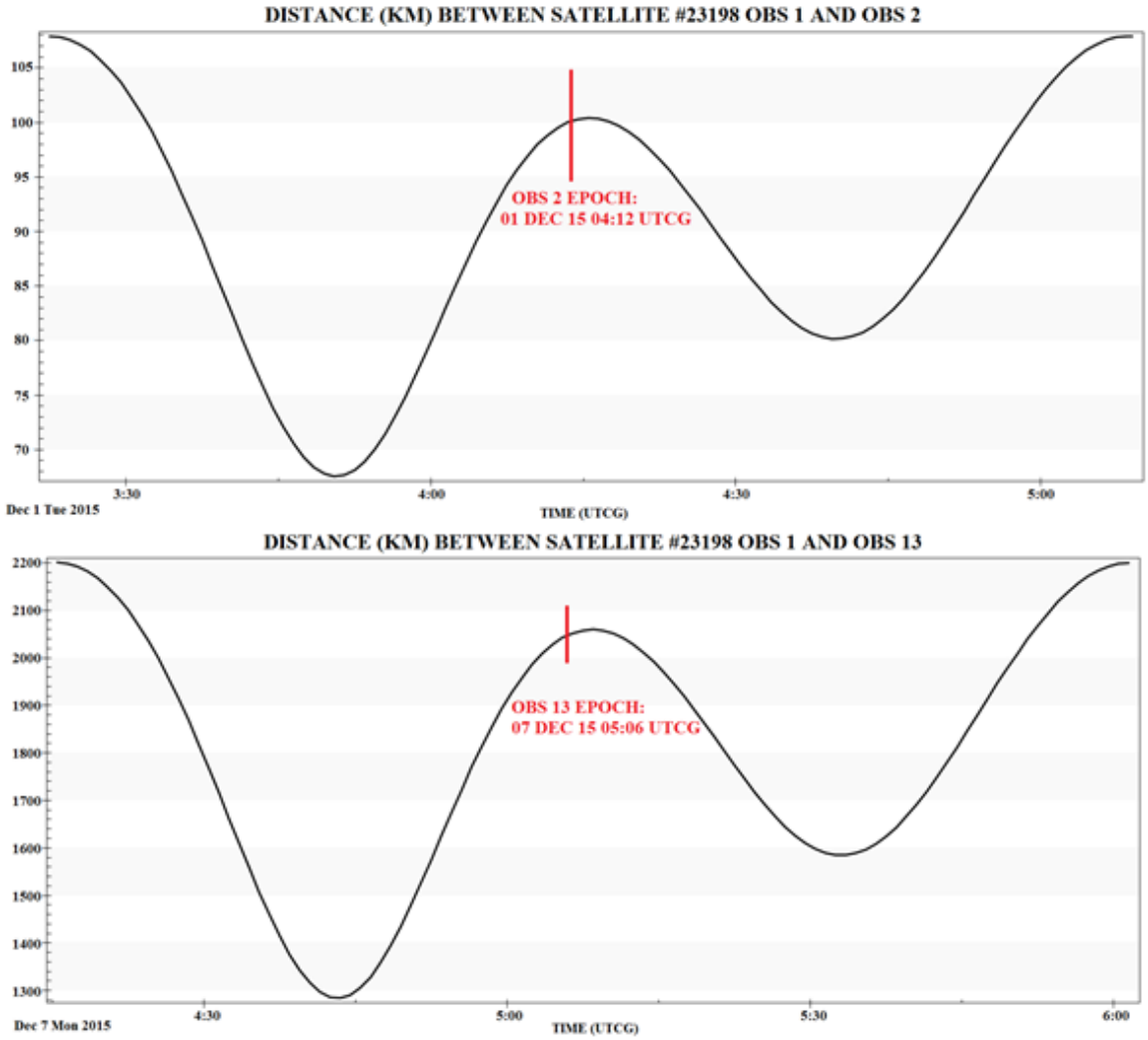

Figure 11. Propagated Error Distance Between #23198 Obs 1 and Obs 2 and 13

Adapted from [29]: *Systems Tool Kit*, version 10.1.0. Analytical Graphics, Incorporated, Exton, PA, 2016.

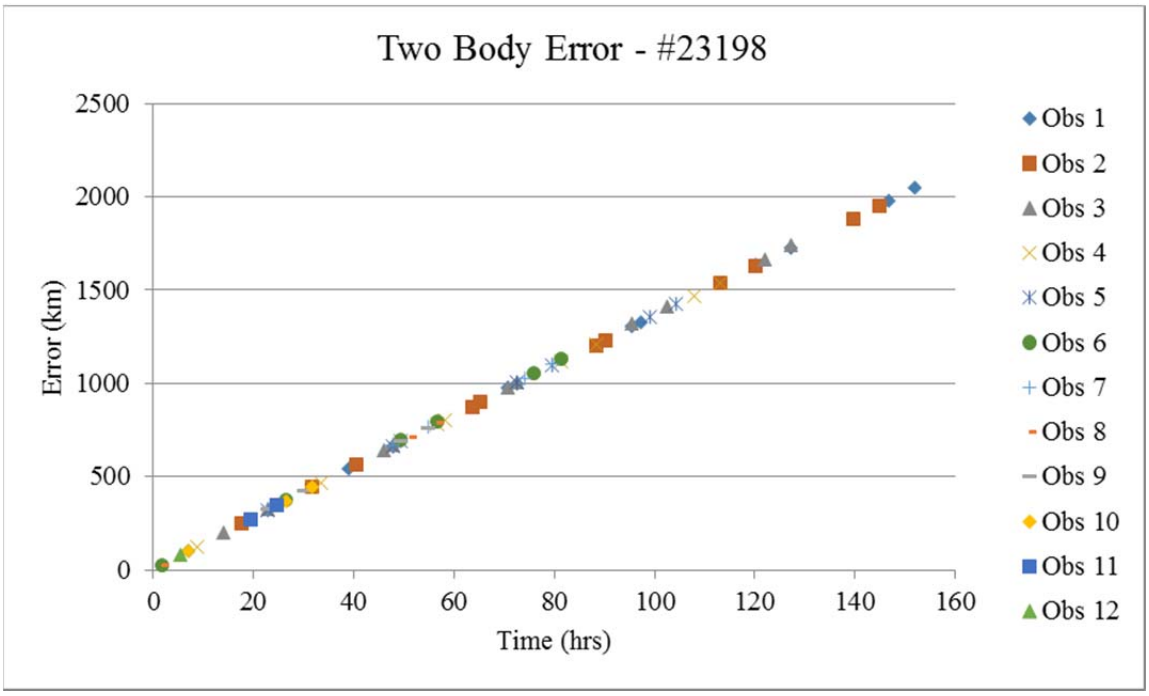

Figure 12. Error of the Two-Body Propagator with Consistent Measurement Locations

However, some satellites have TLE observations generated when the satellite was at differing locations in the orbit, causing the divergent error-rate trend lines demonstrated by Satellite #22161 in Figure 14. In all cases, one of the trend lines correlated more closely with the anticipated slope than the others. Only the values associated with the trend line most consistent with the TLE generation location of the other satellites were used in the final error rate analysis.

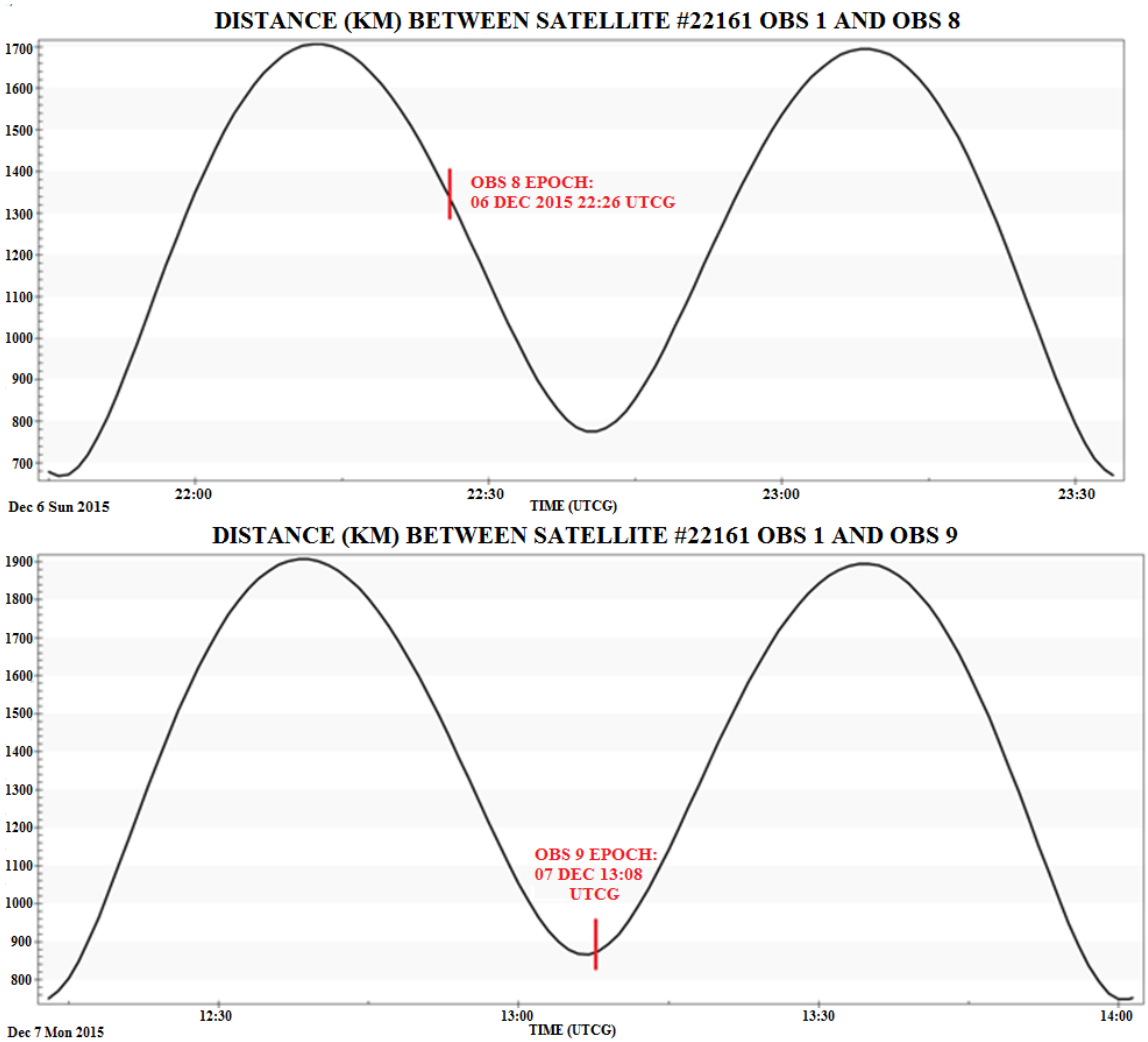

Figure 13. Propagated Error Distance Between #22161 Obs 1 and Obs 8 and 9

Adapted from [29]: *Systems Tool Kit*, version 10.1.0. Analytical Graphics, Incorporated, Exton, PA, 2016.

Figure 14. Error of the Two-Body Propagator with Inconsistent Measurement Locations

In an effort to begin mapping the relationship between altitude, inclination, and error rate, Figure 15 was developed using MATLAB to create an interpolative mesh. Further simulations exploring the uncharted portions will help fill in the mesh and collective understanding. In the meantime, while two-body propagators have been shown to accumulate error much too quickly to be useful over long durations, they should still be considered for short-term duty cycle applications. Depending upon mission requirements and orbit properties, relying on a two-body propagator for 45-60 minutes would still yield power savings between 97.8-98.3% for a receiver with a one-minute cold start. A discussion of potential concepts of operation is discussed in the following chapter.

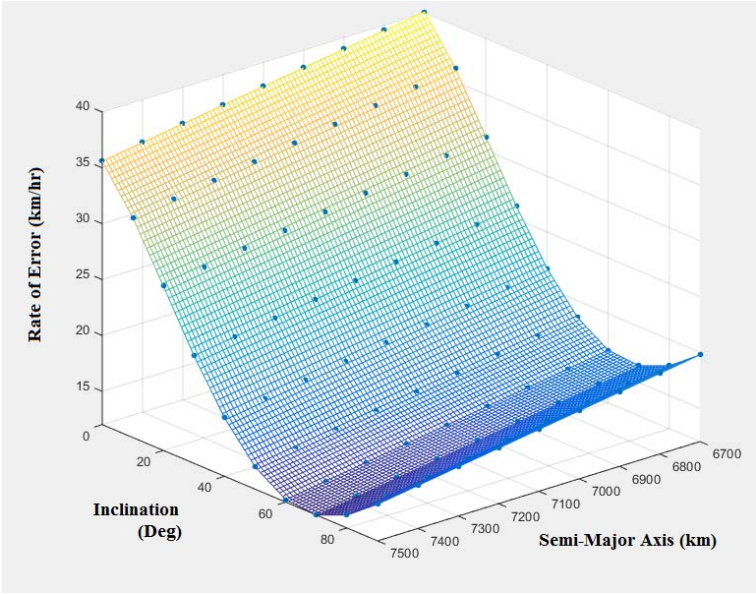

Figure 15. Three Dimension Representation of Rate of Error as a Function of Inclination and Semi-Major Axis

Source: [42] *MATLAB*, version R2014b 8.4.0, MathWorks, Natick, MA, 2014.

C. SGP-4 PROPAGATOR

The same 87 space objects identified for the two-body trials were used again for the SGP-4 propagation error tests. TLE data from the JSPOC was downloaded via the AGI server and set into separate STK satellites representing individual epochs. As in the two-body trials, each of these satellites were propagated to the epoch times of subsequent TLEs and the distance between the propagated satellite and the satellite representing the objects measured position at that time was recorded.

Due to the incorporation of an atmospheric model and a gravity model representative of the Earth's oblateness in SGP-4, there was an expectation that any changes in error rate would be small. However, what was not expected was the highly individual nature of each TLE. In the two-body propagator trials, each satellite gained error uniformly such that a common characteristic could be compared across the satellites. In the SGP-4 tests, each TLE gained error at a different rate than other TLEs for the same object. The resulting conclusion is that the largest source of error in SGP-4 comes from error of inputs to the propagator from the TLE, similar to the old saying, "Garbage in equals garbage out."

Further investigation pointed to the B* term, the modified ballistic coefficient, as the likely culprit, although no defined relationship was evident. Between the TLEs most elements tend to move in one direction, the mean motion usually increases, eccentricity and inclination usually decay, the argument of perigee and RAAN move left or right. However, the resulting differences in error rate did not follow the same patterns. The second TLE may have a greater rate of error than the first and a third may be less than both its predecessors. SGP-4 does not use the first or second derivatives of mean motion from the TLE, meaning the B* term must be the input factor determining the error rate response.

This is plausible considering the large role B* has in the SGP-4 propagator. B* is the sole term for the response of an object through the SGP-4 atmospheric model. It includes the atmospheric scale height, the coefficient of drag, and the object's frontal area all in one term.

$$B^* = \frac{\rho C_D A}{2m} \tag{14}$$

where

ρ = reference value of atmospheric density

C_D = coefficient of drag

A = frontal area

m = mass.

Attempts to better characterize the effect that errors in B* had on the error of the propagator output were unsuccessful. A better understanding of the math and programming inside the propagator are required to define the relationship mathematically. There was some correlation found between the B* term and the shape of the plot of a TLE's error over time. Most of these plots take a parabolic form. Using Microsoft Excel's LINEST function, a second-order polynomial line of best fit could be applied to these plots. Each of the plotted polynomial lines fit the corresponding curve with R^2 values greater than 0.94. For these polynomials of the form $a*x^2+b*x+c$, the first term *a* determines the shape of the plot. Starting with the B* term corresponding

with the lowest *a* curve, or the plot with the lowest rate of error, it was found that as B* differs from this point, there is a non-uniform increase in the *a*-term. Table 2 and Figures 16 and 17 are provided to better illustrate this discussion.

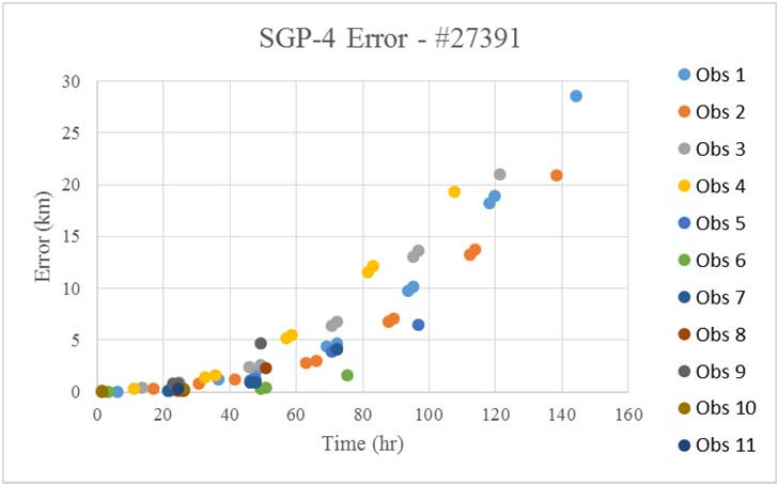

Figure 16. Plot Demonstrating the Variance Between TLEs

These are the error plots for each TLE of object #27391. Notice the parabolic form of each error plot.

Table 2. B* Difference Compared to LINEST 1st Term Values

#27391		B*	LINEST	
Obs	B*	Difference	1st Term	R^2
1	15397-3	3.51E-05	0.0017912	0.998
2	14831-3	2.95E-05	0.0015784	0.998
3	14923-3	3.04E-05	0.0017061	0.998
4	14978-3	3.09E-05	0.0017488	0.998
5	13622-3	1.74E-05	0.0005654	0.986
6	11886-3	0	0.0004692	0.947
7	11342-3	-5.44E-06	0.0019486	0.999
8	11678-3	-2.08E-06	0.0016751	0.999
9	10815-3	-1.07E-05	0.0056218	1

Only the first nine TLEs of #27391 were used for concern that later observations with less data points offered less information to determine their true parabolic form. Here Microsoft Excel's LINEST function returns the first term of the parabolic line of best fit and corresponding R2 term describing the strength of correlation. Notice the smallest 1st term (highlighted) belongs to Obs 6, which had the smallest rate of error in Figure 16. B* Difference is the difference between an Obs B* and that of Obs 6 B*.

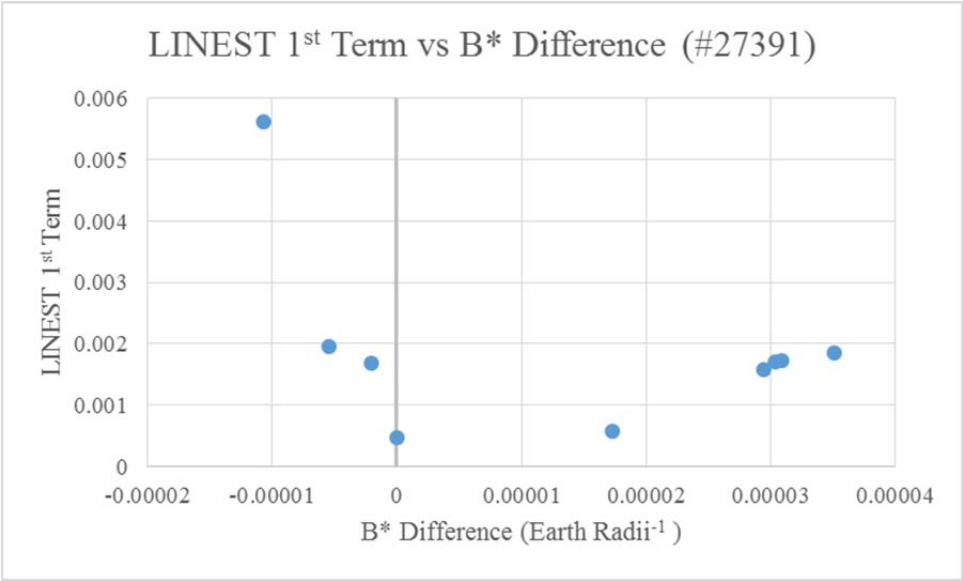

Figure 17. Plot of the First Term of the Best Fit Polynomial Versus the TLE Drag Term's Difference from the Most Accurate TLE's Drag Term

This is a plot of the data from Table 1. Here the Obs 6 B* term is shown at the origin. As the B* of other TLEs differ from the Obs 6 B*, the term describing the shape of the error rate also increases. This does not mean that the B* of the Obs 6 TLE is correct, only that it is the closest of these TLEs in this sample set.

D. SUMMARY

The inability to characterize the error rate of the more accurate SGP-4 propagator to predict its future use is a disappointment. However, because of the parabolic nature of these error rate plots, it reaffirms the safety of using a propagator over short time periods. Relative to the two-body propagator, which would have to be updated at intervals of less than an hour, an SGP-4 propagator could be reasonably employed for approximately a day without sacrificing mission effectiveness. Further, if a satellite operator were to accurately determine atmospheric scale height, coefficient of drag and the frontal area of the satellite and its designed orbit, thus determining their own B* term, it would be feasible to expect sufficient accuracy to operate multiple days without a GPS update.

THIS PAGE INTENTIONALLY LEFT BLANK

VII. APPLICATION

Many small satellite operators are already utilizing this concept of duty cycling the GPS receiver as a means of saving power. Two such satellites are NPSAT1 from the Naval Postgraduate School and NASA's Edison Demonstration of Small Satellite Networks (EDSN).

A. NPSAT1

NPSAT1 uses a SpaceQuest GPS-12 receiver capable of tracking up to 12 channels. This unit has a cold start time of two minutes, meaning that the unit has to download fresh almanac and ephemeris data from the satellites before it can acquire a positional fix. Instead of continuous operation, the unit will power up once every hour, provide a state vector and then power down. By duty cycling, the GPS receiver on NPSAT1 consumes approximately 4% of the 1.5 W of power required to provide continuous updates. Over the remainder of the hour, the onboard Keplerian propagator will predict NPSAT1's position with errors within the navigational requirements of the satellite. In the event the GPS receiver fails, two-line element sets can be uploaded to the satellite from the ground for use in a SGP-4 propagator [2].

If NPS chose to rewrite the SGP-4 propagator in NPSAT1 such that it would accept a GPS state vector in addition to a TLE as input, it could safely propagate an entire day without requiring an update. As an example, a 24-hour duty cycle would result in a 96% increase in efficiency over the current propagation scheme at similar or better positional accuracies. This would decrease the startups and shutdowns of the receiver by 95%. Figures 18 and 19 highlight the impact a 24-hour duty-cycling scheme would have on NPSAT1 in each of its three modes of operation: acquisition of three-axis stability, stability acquired running no experiments, and stability acquired running all experiments.

	NPSAT1 Mode of Operation					
	Acquisition		Acq No Exp		Acq All Exp	
Sub-System	W*hr/Orbit	Percentage	W*hr/Orbit	Percentage	W*hr/Orbit	Percentage
EPS	10.38	30.09	10.38	37.10	10.38	30.70
ADCS	11.93	34.58	5.78	20.66	5.78	17.10
GPS	2.36	6.84	2.36	8.43	2.36	6.98
C&DH	9.83	28.49	8.99	32.13	12.63	37.36
SMS	0	0	0.47	1.68	0.44	1.30
CERTO	0	0	0	0	2.21	6.54
VISIM	0	0	0	0	0.01	0.03
Total	**34.5**	**100**	**27.98**	**100**	**33.81**	**100**

Table 3. NPSAT1 Average Power Usage Without Duty-Cycling GPS

	NPSAT1 Mode of Operation					
	Acquisition		Acq No Exp		Acq All Exp	
Sub-System	W*hr/Orbit	Percentage	W*hr/Orbit	Percentage	W*hr/Orbit	Percentage
EPS	10.38	32.29	10.38	40.51	10.38	33.00
ADCS	11.93	37.12	5.78	22.56	5.78	18.38
GPS	0.002	0.01	0.002	0.01	0.002	0.01
C&DH	9.83	30.58	8.99	35.09	12.63	40.16
SMS	0	0.00	0.47	1.83	0.44	1.40
CERTO	0	0.00	0	0.00	2.21	7.03
VISIM	0	0.00	0	0.00	0.01	0.03
Total	**32.142**	**100**	**25.622**	**100**	**31.452**	**100**

Table 4. NPSAT1 Average Power Usage With a 24-Hour Duty-Cycling Period of the GPS Receiver

A potential concept of operations for duty-cycling GPS receivers on NPSAT1 and other satellites is outlined in Figure 20. Once position and velocity data age has passed a user-defined threshold, the satellite would start a process to be refreshed with new information. The first step is to start the onboard GPS receiver and begin the cold-start process. The receiver would then download fresh almanac and ephemeris data from the GPS satellites before providing its first fix. That information would be translated into orbital elements expressed in a TLE format sent to a SGP-4 propagator in a process explained by P. C. Leopold in his 2014 Master's Thesis "Development of Navigation Solutions for NPSAT1" [43]. The GPS receiver would then be turned off until the next cycle.

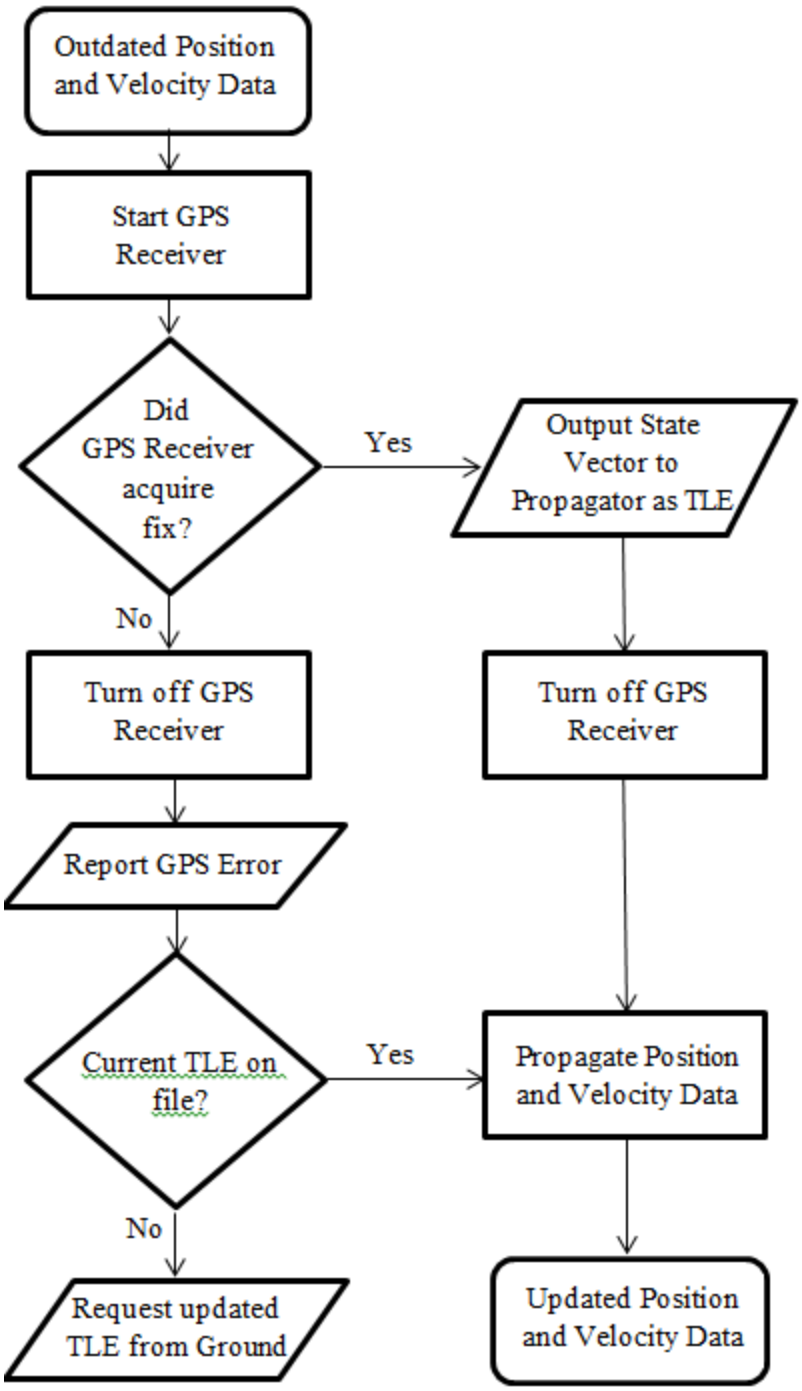

Figure 18. Proposed Concept of Operations for Duty-Cycling GPS Receivers

Failure of the GPS receiver to download almanac and ephemeris data or provide position and velocity data in a time appropriate for the receiver model would flag an error to be reported to the ground station. As a form of redundancy, TLEs periodically

uploaded to the satellite can be used to propagate the satellite's position and velocity in case of GPS failure.

B. EDISON DEMONSTRATION OF SMALL SATELLITE NETWORKS

The NASA Ames Research Center built the satellites of the Edison Demonstration of Small Satellite Networks (EDSN) mission as a group of eight 1.5U Cubesats designed to fly as a networked swarm. Each satellite is equipped with a Samsung Nexus S smartphone processor and a Novatel OEMV-1 model GPS receiver. The GPS receiver provides a fix to the processor at roughly 25-hour intervals, which then propagates the orbit for the following 50 hours and schedules the satellite's activities [44]. The propagator uses a simple atmospheric and J2 gravity model to achieve this level of accuracy. The Novatel receiver requires a sixty-second cold start to the first fix, meaning the EDSN satellites would use less than 0.07% of the 1.1 W for continuous updates [45]. This level of efficiency is imperative because the satellite solar panels provide only one watt of power.

C. ONBOARD PROPAGATION: NOT FOR EVERY MISSION

There are missions for small satellites that will not be able to utilize this concept as a means to power savings. Onboard propagation requires sacrificing the exquisite level of confidence in position and velocity data available from GPS receivers in order to apply limited power to another load. In these missions, such a trade would be a detriment to the satellite's ability to accomplish its task. For example, operations in space science may require that a satellite, or a swarm of satellites, be able to measure and detect changes over short distances in order to map some effect or phenomenon. This type of mission would require that exquisite positional data not available by propagation. Manufacturers and operators may need to identify other creative solutions to save power in these situations. A hybrid approach may be a suitable alternative in these situations; where the GPS receiver is on continuously during operations requiring increased positional information data, then returned to a duty cycle mode when positional knowledge requirements are relaxed.

D. APPLICATION ON FUTURE SATELLITES

This concept is ripe for use on a wide array of small satellites. As satellites continue to get smaller, operators and manufacturers will need to develop and utilize as many power savings concepts as possible. Some may wonder if it is worth the trouble as power savings are only 1–2 W. On satellites capable of producing sufficient power, this concept is likely not useful. However, on small satellites that struggle to produce the power necessary to run all of its hardware, duty cycling all unnecessary electronics is critical to mission success. Consider again the EDSN satellites, whose GPS receiver's power consumption was nearly equal to the power generation capacity of their solar cells.

The power savings from duty cycling GPS receivers can be applied in a variety of ways. Instead of a constant burden on the power budget, obtaining GPS fixes at opportunistic times in the orbit allows the satellite to dedicate power to more essential components. Space science satellites may then be able to run experiments in parallel to gather more data, or technology demonstration satellites might have the capacity to test additional equipment. An educational satellite might accommodate additional functions, allowing students more opportunities to benefit. Every satellite can benefit from a little extra power; duty cycling GPS receivers is one way to deliver extra power without purchasing additional solar capability.

THIS PAGE INTENTIONALLY LEFT BLANK

VIII. CONCLUSIONS AND FUTURE WORK

Duty cycling the GPS receiver has been shown to be an effective way to more efficiently utilize every watt available to small satellites on orbit. The technique is currently being applied in some satellites and should soon proliferate widely to all satellites starved for power. Operators implementing propagators for position and velocity data should opt for the most rigorous propagation method in order to maximize power savings.

While the Two-Body propagator's response to altitude and inclination changes have been sufficiently mapped, the steep error rate incumbent in the Two-Body propagator limits it use. This drives the need to better characterize the SGP-4 propagation method in order to accurately define the upper limit of the time this method can be considered a reliable solution. As processing power available in small components increases, similar analysis can be given to the implementation of the HPOP method as an on-orbit propagator.

Additionally, there is an opportunity to dovetail the findings of this thesis with the Navigation Solution developed by P. C. Leopold for implementation on NPSAT1 and future satellites. Above all, future efforts should continue to think beyond traditional methods to devise creative new solutions to satellite power.

THIS PAGE INTENTIONALLY LEFT BLANK

APPENDIX: SATELLITES BY EXPERIMENT

Varying Altitude	Varying Inclination	Varying Eccentricity
Near Circular Eccent. (< 0.01)	Altitude 500–875 km	Altitude 1122–1222 km
Near Polar Incline (80°-100°)	Near Circular Eccentricity(< 0.01)	Inclination 55°-75°
Semi Major Axis–6700 km	**Inclination 0–10°**	**Eccentricity 0–0.01**
#27391–GRACE 1	#26562–PEGASUS R/B	#10462–SCOUT D-1 R/B
#27392–GRACE 2	#33393–DEMOSAT/FALCON 1	#10579–COSMOS 970 DEB
#28642–DART	#38358–NUSTAR	#12867–COSMOS 970 DEB
6800 km	**10 -20°**	#19562–COSMOS 1823 DEB
#26365–SIMSAT 1	#37839–JUGNU	**0.01–0.02**
#26366–SIMSAT 2	#37841–SRMSAT	#12942–COSMOS 970 DEB
#39451–SWARM B	#37842–PSLV R/B	#37379–JASON DEB
6900 km	**20–30°**	**0.02–0.03**
#24873–IRIDIUM 921	#22489–OXP 1	#00355–THOR ABLESTAR DEB
#24925–DUMMY MASS 1	#25504–SCD 2	#03908–COSMOS 249 DEB
#25527–IRIDIUM 2	#25791–FUSE 1	#13132–N-1 DEB
7000 km	**30–40°**	**0.03–0.04**
#20607–MACSAT 1	#01641–OV2-1	#00643–THOR ABLESTAR DEB
#20608–MACSAT 2	#01642–TITAN 3C DEB	#01942–THOR ABLESTAR DEB
#28230–GP-B	#06153–OAO 3	#05763–COSMOS 397 DEB
7100 km	**40–50°**	**0.04–0.05**
#25287–IRIDIUM 64	#00162–TIROS 3	#10566–COSMOS 970 DEB
#25288–IRIDIUM 65	#00226–RANGER 2	#20174–THOR ABLESTAR DEB
#25777–IRIDIUM 14	#25484–PEGASUS R/B	#35646–COSMOS 2251 DEB
7200 km	**50–60°**	**0.05–0.06**
#00801–TRANSIT 9	#00716–TIROS 6	#13517–SL-8 DEB
#02176–TRANSIT 13	#02088–SCOUT X-4 DEB	#19024–COSMOS 397 DEB
#05397–OV1-21	#29006–TIROS 6 DEB	#34028–COSMOS 2251 DEB
7300 km	**60–70°**	**0.06–0.07**
#00900–CALSPHERE 1	#18665–COSMOS 1900	#03784–COSMOS 252 DEB
#01510–DODECAPOLE 2	#21126–SL-3 DEB	#03794–COSMOS 249 DEB
#17070–POLAR BEAR	#27606–LATINSAT B	#03923–COSMOS 249 DEB
7400 km	**70–80°**	**0.07–0.08**
#00705–TRANSIT 5E 3	#01814–FR 1	#05197–COSMOS 397 DEB
#00902–CALSPHERE 2	#04071–SL-8 R/B	#22161–FREJA
#19420–OSCAR 31	#04369–COSMOS 332	#29256–SL-24 DEB
7500 km	**80–90°**	**0.08–0.09**
#12458–NOVA 1	#20608–MACSAT 2	#03557–COSMOS 252 DEB
#15362–NOVA 3	#25490–TAURUS R/B	#09963–COSMOS 886 DEB
#19223–NOVA 2	#28230–GP-B	#18431–COSMOS 252 DEB
	90–100°	**0.09–0.1**
Most Like NPSAT1's Orbit	#31118–SAUDISAT 3	#09650–COSMOS 886 DEB
#25504–SCD-2	#37789–NIGERIASAT 2	#19112–COSMOS 886 DEB
	#39766–ALOS 2	#23198–APEX R/B

THIS PAGE INTENTIONALLY LEFT BLANK

SUPPLEMENTAL

This supplemental information contains the orbital element and propagation positional error data for each of the 85 satellite objects used in the Altitude, Inclination and Eccentricity experiments, arranged by the JSPOC catalog number of the object. Each object lists the TLEs used in creating the SGP-4 satellites in STK that were obtained via the Space-Track.org catalog or the AGI server. Following the TLEs are the correlating orbital elements used in creating the two-body satellites in STK.

The measured distance between the propagated satellite and the observed positions of the actual body at later epochs is organized by the propagated observation. This was done so that the reader can easily follow the growth in error of each propagation over time for both the SGP-4 and two-body satellites. Graphs showing the same information pictorially are included immediately following the tabled information.

Interested readers should contact the Dudley Knox Library at the Naval Postgraduate School to obtain access to this information.

THIS PAGE INTENTIONALLY LEFT BLANK

LIST OF REFERENCES

[1] NASA. (2007). *Sputnik: The fiftieth anniversary* [Online]. Available: http://history.nasa.gov/sputnik/

[2] H. Helvajian and S.W. Janson, *Small Satellites: Past, Present, and Future,* El Segundo, CA: The Aerospace Corporation, 2008.

[3] P. B. de Selding. (2009, Jul. 1). *World's largest commercial satellite launched* [Online]. Available: http://www.space.com/6920-world-largest-commercial-satellite-launched.html

[4] NASA. (2015). *About SSTP* [Online]. Available: http://www.nasa.gov/directorates/spacetech/small_spacecraft/smallsat_overview.html

[5] I. Nikolova, "Microsatellites advantages, profitability and return," in *Space, Ecology, and Safety Conf.*, Varna, Bulgaria, 2005. [Online]. Available: http://www.space.bas.bg/sens/Ses2005/SS3.pdf

[6] D. N. Baker, et al., "The large benefit of small satellite missions" *EoS Trans. AGU.* vol. 89, no. 33, Aug. 2008.

[7] NASA. (2016). *Operational Small Explorers (SMEX) missions* [Online]. Available: http://explorers.gsfc.nasa.gov/smex.html

[8] ESA. (2015). *Solar Orbiter overview* [Online]. Available: http://www.esa.int/Our_Activities/Space_Science/Solar_Orbiter

[9] D. Werner. (2013, Oct. 14). *Skybox Imaging's hopes high as launch of first satellites draws near* [Online]. Available: http://spacenews.com/37671commercial-earth-observation-skybox-imagings-hopes-high-as-launch-of-first/

[10] ESA. (2015). *TechDemoSat-1* [Online]. Available: https://directory.eoportal.org/web/eoportal/satellite-missions/t/techdemosat-1

[11] T. Logsdon, *The NAVSTAR Global Positioning System*, New York, NY: International Thomson Publishing, 1992.

[12] M. Slater. (2015, Jun. 25). *GPS: A generation of service to the world* [Online]. Available: http://www.af.mil/News/ArticleDisplay/tabid/223/Article/601748/gps-a-generation-of-service-to-the-world.aspx

[13] DOD, "Global Positioning System Standard Positioning Service Performance Standard," U.S. Dept. of Defense, Washington, DC., Tech. Rep., 2008. [Online]. Available: http://www.gps.gov/technical/ps/2008-SPS-performance-standard.pdf

[14] DOD, "Global Positioning System Precise Positioning Service Performance Standard," U.S. Dept. of Defense, Washington, DC., Tech. Rep., 2007. [Online]. Available: http://www.gps.gov/technical/ps/2007-PPS-performance-standard.pdf

[15] USAF. (2015). *GPS space segment* [Online]. Available: http://www.gps.gov/systems/gps/space/

[16] USAF. (2015). *GPS control segment* [Online]. Available: http://www.gps.gov/systems/gps/control/

[17] J. Gerner, *et al*., "TOPSTAR 3000–An Enhanced GPS Receiver for Space Applications," *ESA Bulletin,* no. 104, pp. 86–91, Nov. 2000. [Online]. Available: http://www.esa.int/esapub/bulletin/bullet104/gerner104.pdf

[18] USAF. (2015). *New civil signals* [Online]. Available: http://www.gps.gov/systems/gps/modernization/civilsignals/#L1C

[19] R. J. Cosentino, D. W. Diggle, "Differential GPS," in *Understanding GPS Principles and Application*, E. D. Kaplan, Ed. Boston, MA: Artech House, 1996 pp. 375-376.

[20] B. Hofmann-Wellenhof, H. Lichtenberger, and J. Collins, *GPS Theory and Practice*, 5th ed. Austria: Springer-Verlag/Wein, 2001.

[21] NSTB/WAAS T&E Team, "Global Positioning System (GPS) Standard Positioning Service (SPS) performance analysis report #86," William J. Hughes Tech. Center, FAA, Atlantic City, NJ, Tech. Rep., 2014. [Online]. Available: http://www.nstb.tc.faa.gov/reports/PAN86_0714.pdf#page=22

[22] R. C. Olsen, "Introduction to the space environment", unpublished.

[23] B. Parkinson, J. Spilker, "GPS Error Analysis," in *Global Positioning System: Theory and Applications,* vol. 1, Washington, DC: American Institute of Aeronautics and Astronautics, Inc., 1996, pp. 478–483.

[24] USCG. (1996). *NAVSTAR GPS user equipment introduction* [Online]. Available: http://www.navcen.uscg.gov/pubs/gps/gpsuser/gpsuser.pdf

[25] USCG. (2016). *NDGPS general information* [Online]. Available: http://www.navcen.uscg.gov/?pageName=dgpsMain

[26] NASA. (2015). *The Global Differential GPS (GDGPS) System* [Online]. Available: http://www.gdgps.net/system-desc/index.html

[27] FAA. (2015). *Wide Area Augmentation System–how it works* [Online]. Available: http://www.faa.gov/about/office_org/headquarters_offices/ato/service_units/techops/navservices/gnss/waas/howitworks/

[28] H. Curtis, *Orbital Mechanics for Engineering Students,* 3rd ed. Oxford, UK: Elsevier, 2014.

[29] *Systems Tool Kit*, version 10.1.0. Analytical Graphics, Incorporated, Exton, PA, 2016.

[30] University of Nebraska-Lincoln. (2015). *Kepler's laws of planetary motion* [Online]. Available: http://astro.unl.edu/naap/pos/pos_background1.html

[31] NASA. (2014). *Voyager: The interstellar missions* [Online]. Available: http://voyager.jpl.nasa.gov/science/hyperbolic.html

[32] J. J. Sellers. (2015). *Inclination* [Online]. Available: http://www.agi.com/resources/educational-alliance-program/astro-primer/primer65.htm

[33] J. J. Sellers. (2015). *STK propagators* [Online]. Available: http://www.agi.com/resources/educational-alliance-program/astro-primer/primer102.htm

[34] E. Fantino. (2011). *Orbits and propagators* [Online]. Available: https://www.agi.com/resources/educational-alliance-program/curriculum_exercises_labs/ETSEIAT_2011_2012/DVE1_2011_T07__Orbits_STK.pdf

[35] O. Montenbruck and E. Gill, *Satellite Orbits: Models, Methods, Applications,* 3rd ed. Germany: Springer-Verlag, 2005.

[36] M. H. Lane, F. R. Hoots, "General Perturbations Theories Derived from the 1965 Lane Drag Theory," Aerospace Defense Command, United States Air Force, Peterson AFB, CO, Tech. Rep. Special Astrodynamic Report No. 2, Dec. 1979.

[37] AGI. (2015). *STK 10 help* [Online]. Available: http://www.agi.com/resources/help/online/stk/10.1/index.html?page=source%2Fstk%2FvehSat_orbitProp_msgp4.htm

[38] T. S. Kelso. (2014). *Frequently asked questions: Two-line element set format* [Online]. Available: http://www.celestrak.com/columns/v04n03/

[39] NASA. (2011). *Definition of two-line element set coordinate system* [Online]. Available: http://spaceflight.nasa.gov/realdata/sightings/SSapplications/Post/JavaSSOP/SSOP_Help/tle_def.html

[40] T. S. Kelso, "Validation of SGP4 and IS-GPS-200D Against GPS Precision Ephemerides," in *17th AAS/AIAA Space Flight Mechanics Conference*, Sedona, AR, 2007.

[41] M. J. Muolo, *Space Handbook*, vol. 2, Maxwell AFB, AL: Air University, 1993.

[42] *MATLAB*, version R2014b 8.4.0, MathWorks, Natick, MA, 2014.

[43] P. C. Leopold, "Development of Navigation Solution for NPSAT1," M.S. thesis, Space Systems Academic Group, Naval Postgraduate School, Monterey, CA, 2014.

[44] J. Hanson et al., "The EDSN Intersatellite Communications Architecture" in *Small Satellites Conference*, Logan, UT, 2014.

[45] *OEMV Family Installation and Operation User Manual,* Rev. 13, Novatel, Calgary, Canada, 2010.

INITIAL DISTRIBUTION LIST

1. Defense Technical Information Center
   Ft. Belvoir, Virginia

2. Dudley Knox Library
   Naval Postgraduate School
   Monterey, California